Supplementary Information for

Ultrasound drives chemical systems out of equilibrium

Marcus Lantzius-Beninga[a,b], Gurudas Chakraborty[b]*, Chen Li[b], Jens Köhler[b], and Andreas Herrmann[a,b]*

a Institute of Technical and Macromolecular Chemistry, RWTH Aachen University, Aachen, Germany

b DWI – Leibniz-Institute for Interactive Materials, Aachen, Germany

* Correspondence and requests for materials should be addressed to Gurudas Chakraborty chakraborty@dwi.rwth-aachen.de or Andreas Herrmann herrmann@dwi.rwth-aachen.de.

Table of contents

1. Synthetic details

1.1. Synthesis of acridinium perchlorate, disulfide polymer, and thiol-selective probe

Synthesis of acridinium perchlorate[1]

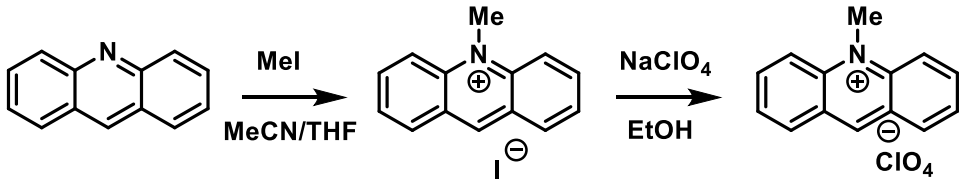

Acridine (1.67 mmol, 300 mg) was dissolved in a mixture of acetonitrile and tetrahydrofuran (4 mL, 1:1 v/v), and methyl iodide (16.7 mmol, 10 eq., 2.370 g) was added. The resulting solution was stirred for 3 d. All volatiles were removed under reduced pressure, the resulting solid was re-dispersed in acetonitrile, and the liquid phase was separated. The solvent was removed and the resulting residue was washed with pentane (50 mL) five times. The obtained product was dried yielding a red solid (1.09 mmol, 65%). ^{1}H NMR (400 MHz, DMSO-d_6): δ 10.19 (s, 1H), 8.80 (d, 2H), 8.66 (d, 2H), 8.46 (t, 2H), 8.03 (t, 2H), 4.86 (s, 3H) ppm. ^{13}C NMR (101 MHz, DMSO-d_6) δ 150.9, 139.2, 131.7, 127.8, 126.3, 119.0, 38.9 ppm.

Acridinium iodide (1.09 mmol, 350.1 mg) was dissolved in a mixture of acetonitrile and ethanol (20 mL, 1:1 v/v) and stirred with a basic Amberlite IRA67 ion exchange resin for 30 min. Afterwards, the solvent was evaporated and the solid re-dissolved in ethanol (6 mL). Sodium perchlorate (1.09 mmol, 133.0 mg) was added and the product precipitated from the solution. After 16 h, the product was filtered and washed with ethanol, yielding a yellow-to-brown solid (1.09 mmol, quant.) ^{1}H NMR (400 MHz, $CDCl_3$) δ 8.52 (d, 2H), 7.69 (t, 2H), 7.50 (d, 2H), 7.23 (t, 2H), 3.86 (s, 3H) ppm.

Synthesis of disulfide polymer

The linear oligo(ethylene glycol methyl ether) acrylate (OEGA) polymer containing a chain-centered disulfide mechanophore was synthesized by Cu-mediated controlled radical polymerization. Bis(2-(2′-bromoisobutyryloxy)ethyl)disulfide (0.01 mmol, 4.5 mg), Me_6TREN (0.001 mmol, 0.23 mg), purified OEGA (10 mmol, 1000 eq., 4.80 g, see Methods for purification details), and copper(II) bromide (0.13 µmol, 0.03 mg) were dissolved in anhydrous dimethyl sulfoxide (4 mL) and a pre-activated copper wire (3 cm, see Methods) was placed above the reaction mixture. The resulting mixture was

degassed by four cycles of freeze-pump-thaw and the polymerization was initiated by releasing the copper wire into the solution. After 16 h, the mixture had turned highly viscous and the reaction was terminated by exposure to air. The crude product was repeatedly precipitated in ice-cold diethyl ether (200 mL) and the resulting viscous product was dried (4.35 g, 91%). SEC (THF): M_n = 106 kg·mol^{-1}, $Đ$ = 1.1 (Supplementary Fig. 41).

Synthesis of thiol-selective probe[2]

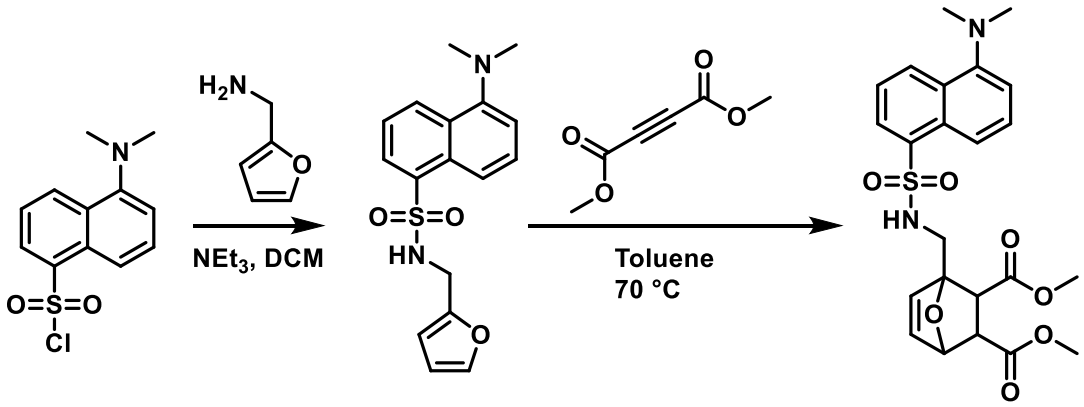

Dansyl chloride (1.85 mmol, 500.0 mg) was dissolved in anhydrous DCM (7.5 mL) and anhydrous NEt_3 (0.5 mL). To this solution, furfurylamine (1.95 mmol, 1.05 eq., 188.9 mg) in anhydrous DCM (2.5 mL) was added dropwise. The solution was stirred for 3 h before adding the reaction mixture to water (30 mL). The organic phase was separated, dried with magnesium sulfate and all volatiles were removed under reduced pressure. The crude product was purified by column chromatography (silica, pentane/ethyl acetate 1:1) yielding the product as a yellow oil (1.69 mmol, 91%). ^{1}H NMR ($CDCl_3$, 300 MHz): δ 8.52 (d, 1H), 8.21 (m, 2H), 7.52 (pent., 2H), 7.16 (d, 1H), 7.04 (s, 1H), 6.03 (m, 1H), 5.87 (m, 1H), 4.13 (s, 2H), 2.88 (s, 6H) ppm.

The dansyl furfuryl fluorophore (0.61 mmol, 200 mg) and acetylenedicarboxylic acid (0.61 mmol, 1 eq., 70 mg) were submitted to a pressure tube and dissolved in toluene (2.5 mL). The mixture was heated to 70 °C for 20 h. Afterwards, the solvent was removed and the crude product was purified by column chromatography (silica, pentane/ethyl acetate 1:5 to 0:5) yielding a yellow solid (0.42 mmol, 72%). ^{1}H NMR ($CDCl_3$, 300 MHz): δ 8.55 (d, 1H), 8.22 (m, 2H), 7.54 (m, 3H), 7.23 (m, 2H), 6.17 (m, 2H), 5.99 (s, 1H), 4.72 (s, 2H), 3.60 (s, 6H), 2.87 (s, 6H) ppm. HR-ESI MS: 473.1386

(clcd. 473.1377 for $M+H^+$), 495.1204 (clcd. 495.1196 for $M+Na^+$), 511.0944 (clcd. 511.0936 for $M+K^+$), 945.2720 (clcd. 945.2681 for $2M+H^+$), 967.2537 (clcd. 967.2501 for $2M+Na^+$), 983.2285 (clcd. 983.2240 for $2M+K^+$).

1.2. Synthesis of naphthalimide fluorophore[3]

Synthesis of bromo naphthylic imide

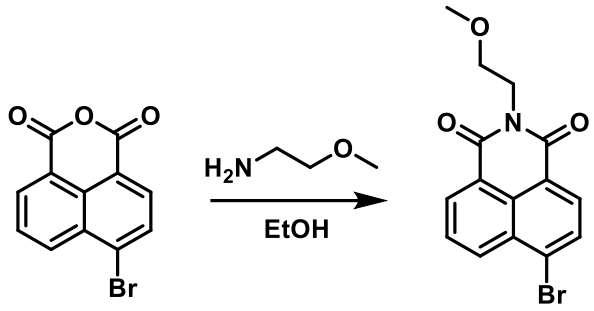

4-Bromo-1,8-naphthylic anhydride (1.80 mmol, 500 mg) and 2-methoxy ethylamine (1.80 mmol, 1.0 eq., 135.5 mg) were dispersed in ethanol (20 mL). The resulting mixture was heated to 60 °C for 4 d. All volatiles were removed yielding the pure product as a brown solid (1.74 mmol, 97%). ^{1}H NMR (400 MHz, $CDCl_3$) δ 8.62 (d, 1H), 8.51 (d, 1H), 8.35 (d, 1H), 7.97 (t, 1H), 7.82 (d, 1H), 4.41 (t, 2H), 3.72 (t, 2H), 3.37 (s, 3H) ppm. ^{13}C NMR (101 MHz, $CDCl_3$) δ 163.8, 163.7, 133.3, 132.2, 131.4, 131.2, 130.6, 130.4, 129.7, 129.1, 128.1, 123,1, 122.2, 69.7, 58.9, 39.5 ppm. The characterization data is in accordance with previously reported data.[3]

Synthesis of naphthalimide tertiary amine

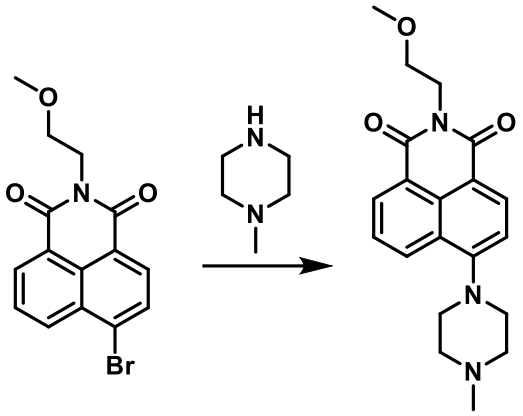

Bromo naphthylic imide (0.60 mmol, 200 mg) and *N*-methyl piperazine (0.90 mmol, 1.5 eq., 90.1 mg) were dispersed in ethanol (6 mL). The mixture was heated under reflux at 85 °C for 2 d. After that, all volatiles were removed and the crude product was purified by column chromatography (silica, dichloromethane/methanol 10:1) yielding the solid product (0.28 mmol, 46%). ^{1}H NMR (400 MHz, $CDCl_3$) δ 8.60 (d, 1H), 8.52 (d, 1H), 8.40 (d, 1H), 7.71 (t, 1H), 7.21 (d, 1H), 4.43 (t, 2H), 3.74 (t, 2H), 3.38 (s, 3H), 3.31 (m, 4H), 2.76 (m, 4H), 2.45 (s, 3H) ppm. ^{13}C NMR (101 MHz, $CDCl_3$) δ 164.8, 164.3, 132.9, 131.4, 130.5, 125.8, 123.3, 120.0, 115.1, 69.9, 58.9, 55.3, 53.1, 46.3, 39.2 ppm.

1.3. Synthesis of perylene monoimide (PMI) fluorophores

Synthesis of PMI[4]

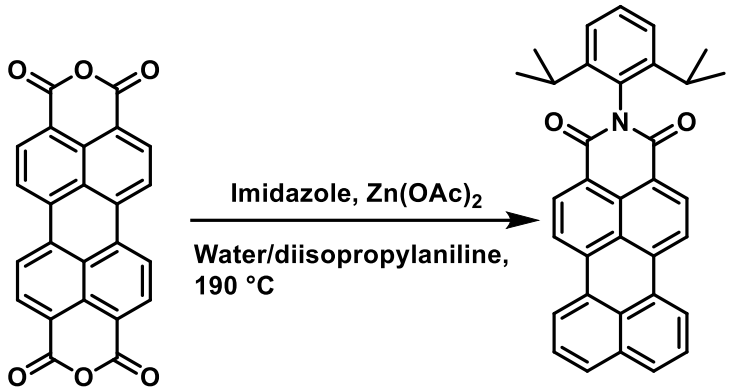

Diisopropyl aniline (1.30 mmol, 0.25 mL), perylenetetracarboxylic dianhydride (2.34 mmol, 1.8 eq., 918.0 mg), zinc acetate dihydrate (1.82 mmol, 1.4 eq., 399.5 mg), and imidazole (70.2 mmol, 54 eq., 4.82 g) were suspended in water (4 mL) in a

pressure tube and heated to 190 °C for 2 d. Afterwards, the resulting solid was filtered and washed with water (4 × 25 mL), 2 M HCl (aq, 25 mL), and a methanol/water mixture (1:1 v/v, 25 mL), before rinsing the resulting solid with dichloromethane. The soluble portion was further purified by column chromatography (first: silica, chloroform/acetone 1:1 to 0:1, second silica, pentane/dichloromethane 1:1 to 0:1) yielding the product as red solid (0.238 mmol, 11% isolated yield). ^{1}H NMR (400 MHz, $CDCl_3$) δ 8.66 (d, 2H), 8.50 (m, 4H), 7.95 (d, 2H), 7.68 (t, 2H), 7.46 (m, 1H), 7.35 (d, 2H), 2.77 (sept., 1H) 1.17 (d, 12H) ppm. ^{13}C NMR (101 MHz, $CDCl_3$) δ 194.4, 164.5, 146.2, 132.6, 131.5, 127.6, 124.5, 124.4, 121.5, 120.7, 29.6, 24.5 ppm. The characterization data is in accordance with previously reported data.[4]

Synthesis of PMI bromide[4]

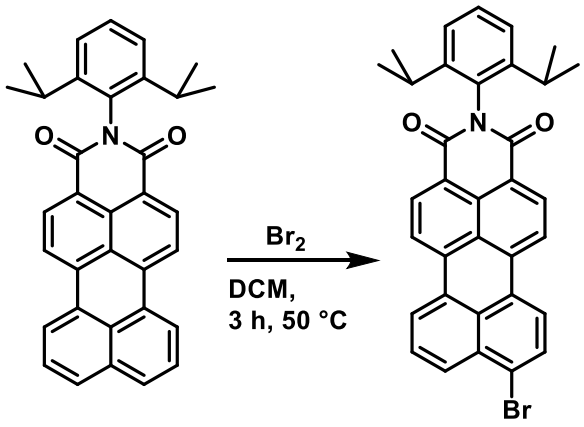

Perylene monoimide (1.25 mmol, 600 mg) was dissolved in anhydrous dichloromethane (20 mL) and bromine (2.5 mmol, 2.0 eq., 400 mg) was slowly added to the solution. The reaction mixture was heated to 60 °C for 3.5 h and was afterwards washed with 10% sodium thiosulfate solution (2 × 20 mL). The organic phase was dried with magnesium sulfate and all volatiles were removed under reduced pressure. The crude product was purified by column chromatography (silica, pentane/chloroform 1:1 to 0:1) yielding the product as red solid (0.90 mmol, 72%). ^{1}H NMR (400 MHz, $CDCl_3$) δ 8.66 (m, 2H), 8.47 (m, 2H), 8.41 (d, 1H), 8.31 (d, 1H), 8.26 (d, 1H), 7.93 (d, 1H), 7.75-7.63 (m, 1H), 7.47 (t, 1H), 7.34 (d, 2H), 2.77 (hept., 2H) 1.13 (d, 12H) ppm. ^{13}C NMR (101 MHz, $CDCl_3$) δ 202.7, 160.0, 145.8, 137.0, 132.3, 132.2, 131.4, 131.1, 128.3, 124.6, 124.2, 124.0, 121.5, 120.9, 120.6, 29.3, 24.2 ppm. The characterization data is in accordance with previously reported data.[4]

Synthesis of PMI primary amine[5]

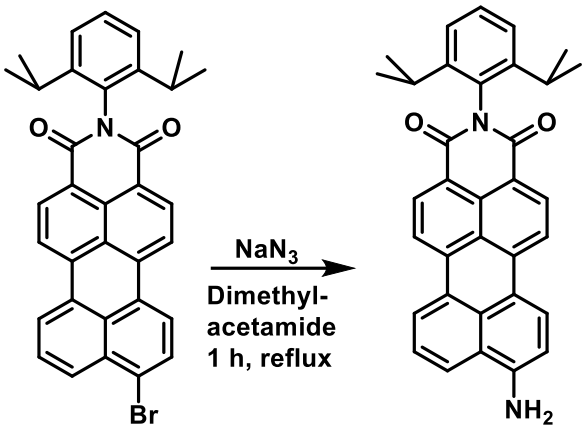

PMI bromide (0.27 mmol, 150 mg) was added to a pressure tube and suspended in *N*,*N*-dimethyl acetamide (10 mL). Sodium azide (8.05 mmol, 30 eq., 523.2 mg) was added and the atmosphere was changed to argon by purging for 5 min. The red mixture was heated to 165 °C for 1 h, with a color shift to blue indicating the formation of the product. The volatiles were removed under reduced pressure and the resulting solid was re-dissolved in dichloromethane. The solution was washed with water (3 × 50 mL) and the organic phase was dried with magnesium sulfate. The crude product was purified by column chromatography (silica, pentane/dichloromethane 1:3 to dichloromethane/tetrahydrofuran 10:1) yielding the product as dark-blue solid (0.10 mmol, 37%). ^{1}H NMR (400 MHz, DMSO-d_6) δ 8.78 (d, 1H), 8.61 (d, 1H), 8.51 (d, 1H), 8.38 (m, 1H), 8.31 (d, 1H), 7.65 (t, 1H), 7.44 (t, 1H), 7.36-7.31 (m, 2H), 7.19 (s, 1H), 6.92 (t, 1H), 6.65 (br, 1H), 2.63 (hept., 2H), 1.08 (d, 12H) ppm. The characterization data is in accordance with previously reported data.[5] HR-ESI MS: 497.2256 m/z (clcd. 497.2224 for $M+H^+$), 519.2060 (clcd. 519.2043 for $M+Na^+$), 535.1812 (clcd. 535.1782 for $M+K^+$), 1015.4236 (clcd. 1015.4194 for $2M+Na^+$).

Synthesis of PMI tertiary amine

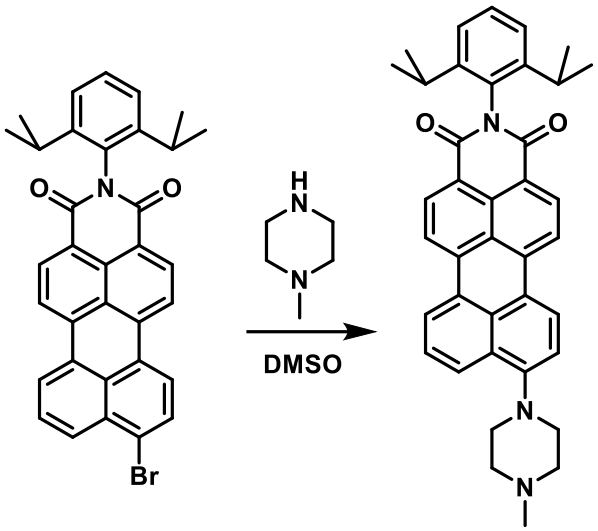

PMI bromide (0.18 mmol, 100 mg) was added to a pressure tube and suspended in dimethyl sulfoxide (4 mL). *N*-Methyl piperazine (1.79 mmol, 10 eq., 179.3 mg) was added and the resulting red suspension was heated to 160 °C for 6 h turning violet. The mixture was added to water (40 mL) and the product was extracted with ethyl acetate (3 × 40 mL). The combined organic phases were dried with magnesium sulfate and the crude product was purified by column chromatography (silica, dichloromethane/methanol 96:4) yielding a violet solid (0.18 mmol, quant.). ^{1}H NMR (400 MHz, $CDCl_3$) δ 8.61 (dt, 2H), 8.48 (m, 1H), 8.42 (m, 2H), 8.34 (m, 1H), 8.24 (d, 1H), 7.65 (t, 1H), 7.45 (t, 1H), 7.34 (d, 2H), 7.22 (d, 1H), 3.28 (m, 4H), 2.80 (m, 4H), 2.78 (m, 2H), 1.17 (d, 12H) ppm. ^{13}C NMR (101 MHz, $CDCl_3$) δ 164.2, 152.9, 145.9, 138.0, 132.3, 132.1, 129.8, 127.0, 126.4, 125.1, 124.3, 124.1, 120.9, 120.0, 119.2, 116.1, 55.5, 53.0, 46.3, 41.1, 29.8, 29.2, 24.2 ppm. HR-ESI MS: 580.2975 (clcd. 580.2958 for $M+H^+$), 602.2789 (clcd. 602.2778 for $M+Na^+$), 618.2527 (clcd. 618.2517 for $M+K^+$), 1159.5865 (clcd. 1159.5844 for $2M+H^+$), 1181.5697 (clcd. 1181.5664 for $2M+Na^+$), 1197.5426 (clcd. 1197.5403 for $2M+K^+$).

1.4. Synthesis of [2]rotaxane

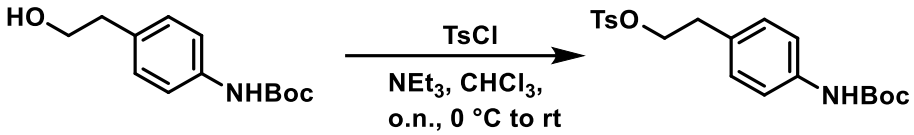

N-Boc-2-(4-aminophenyl) ethanol (4.21 mmol, 1.00 g) was dissolved in chloroform (5 mL) and triethylamine (6.32 mmol, 1.5 eq., 640 mg) was added. The solution was cooled to 0 °C before tosyl chloride (6.32 mmol, 1.5 eq., 1.205 g) in chloroform (5 mL) was added dropwise. The reaction mixture was stirred for 16 h and allowed to warm to room temperature during that time. Afterwards, chloroform (20 mL) was added and the solution was washed with water (3 × 25 mL). The organic phase was dried with magnesium sulfate and all volatiles were removed under reduced pressure yielding the product (4.2 mmol, quant.). ^{1}H NMR (400 MHz, $CDCl_3$) δ 7.67 (d, 2H), 7.27 (d, 2H), 7.24 (d, 2H), 7.02 (d, 2H), 6.43 (br, 1H), 4.16 (t, 2H), 2.91 (t, 2H), 2.43 (s, 3H), 1.51 (s, 9H) ppm. The characterization is in accordance with previously reported data.[6]

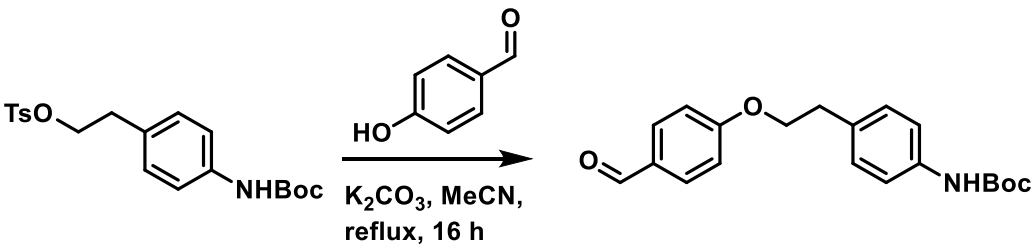

N-Boc-2-(4-aminophenyl) ethyl tosylate (2.1 mmol, 821.4 mg) was added to a pressure tube and dissolved in acetonitrile (10 mL). 4-Hydroxybenzaldehyde (2.3 mmol, 1.1 eq., 280.9 mg) and potassium carbonate (2.3 mmol, 1.1 eq., 317.9 mg) were added. The mixture was stirred at 85 °C for 5 h. After that, the remaining solid was separated and the volatiles were removed under reduced pressure. The solid was re-dissolved in dichloromethane (50 mL) and washed with saturated sodium bicarbonate solution (50 mL) and sodium hydroxide (2 w%) solution (50 mL). The organic phase was dried with magnesium sulfate and all volatiles were removed yielding the solid product (1.5 mmol, 71%). ^{1}H NMR (400 MHz, $CDCl_3$) δ 9.87 (s, 1H), 7.83 (m, 2H), 7.30-7.20 (m, 5H), 6.97 (d, 2H), 6.45 (br, 1H), 4.21 (t, 2H), 3.07 (t, 2H), 1.47 (s, 9H) ppm. The characterization data is in accordance with previously reported data.[6]

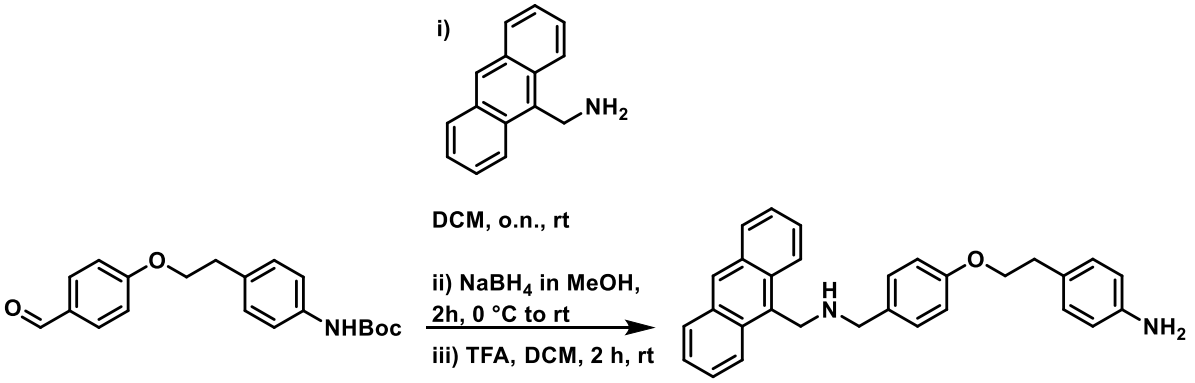

i) Aminomethyl anthracene (0.75 mmol, 155.5 mg) was dissolved in anhydrous dichloromethane (6 mL) and added to pre-activated molecular sieve (0.3 nm). To this solution, tert-butyl (4-(2-(4-formylphenoxy)ethyl)phenyl)carbamate (0.75 mmol, 252.9 mg) in anhydrous dichloromethane (5 mL) was added. The reaction mixture was stirred for 17 h before evaporating all volatiles. The product was directly used in the subsequent reaction step without further isolation. ^{1}H NMR (400 MHz, $CDCl_3$) δ 8.48 (s, 1H), 8.30 (m, 2H), 8.03 (m, 3H), 7.53 (m, 7H), 7.29 (m, 1H), 7.15 (d, 2H), 6.82 (d, 2H), 6.43 (br, 1H), 5.82 (s, 2H), 4.10 (t, 2H), 3.00 (t, 2H), 1.57 (s, 9H) ppm.

ii) The resulting solid (0.75 mmol) was dissolved in anhydrous methanol (7 mL) and cooled to 0 °C. Sodium borohydride (2.02 mmol, 2.7 eq., 76.4 mg) was added and the suspension was stirred at 0 °C for 2 h and at room temperature for 1 h. Subsequently, water (5 mL) was slowly added and all volatiles were removed under reduced pressure. The resulting solid was re-dissolved in dichloromethane (40 mL) and washed with water (2 × 40 mL) and brine (40 mL). The organic phase was dried with magnesium sulfate and all volatiles were removed. Column chromatography (silica, pentane/ethyl acetate 2:3 to 0:1) yielded the product (0.24 mmol, 31%). ^{1}H NMR (400 MHz, $CDCl_3$) δ 8.39 (s, 1H), 8.22 (m, 2H), 7.98 (m, 2H), 7.47 (m, 4H), 7.32 (m, 4H), 7.20 (m, 2H), 6.97-6.89 (dd, 2H), 6.53 (br, 1H), 4.66 (t, 2H), 4.12 (m, 2H), 3.96 (t, 2H), 3.05 (t, 2H), 1.53 (s, 9H) ppm. ^{13}C NMR (101 MHz, $CDCl_3$) δ 158.2, 153.0, 139.5, 136.9, 133.0, 132.5, 132.2, 131.6, 131.4, 131.3, 130.5, 130.4, 129.9, 129.7, 129.6, 129.3, 129.2, 128.7, 127.5, 127.4, 126.2, 125.1, 125.0, 124.3, 124.1, 122.4, 118.9, 114.6, 80.5, 68.9, 53.6, 44.7, 35.2, 28.5 ppm.

iii) After purification and characterization, the solid was dissolved in anhydrous dichloromethane (10 mL) and trifluoro acetic acid (1.2 mL) was added dropwise. The solution was stirred for 5 h and afterwards all volatiles were removed under reduced

pressure. The crude product was re-dissolved in dichloromethane and washed with saturated sodium bicarbonate solution (2 × 30 mL). The organic phase was dried with magnesium sulfate, all volatiles were removed and the product was directly used in the next step without further isolation.

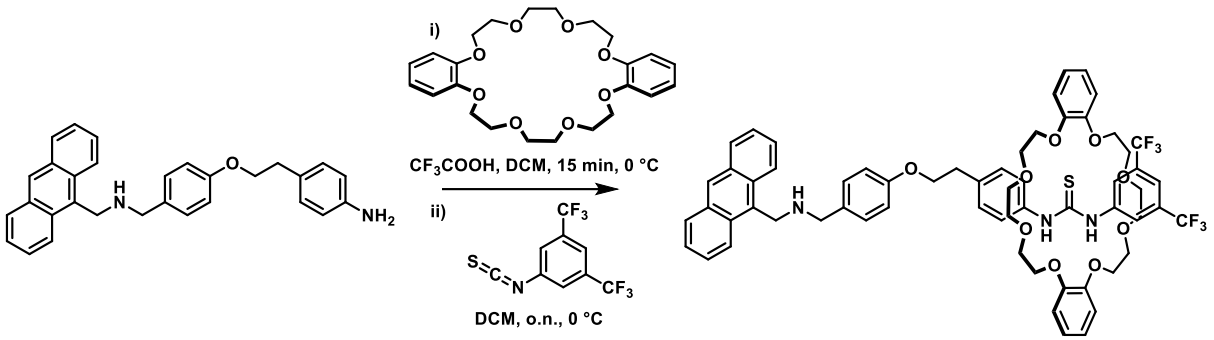

4-(2-(4-(((anthracen-9-ylmethyl)amino)methyl)phenoxy)ethyl)aniline (0.08 mmol) and dibenzo-24-crown-8 (0.24 mmol, 3.0 eq., 107.6 g) were dissolved in anhydrous dichloromethane (3 mL) and the solution was cooled to 0 °C. Trifluoro acetic acid (0.08 mmol, 6.3 µL) was added and the resulting solution was stirred for 20 min. Then, 3,5-bis(trifluoromethyl)phenyl isocyanate (0.12 mmol, 1.5 eq., 22 µL) was added dropwise. The reaction mixture was stirred for 24 h and allowed to warm to room temperature during that time. All volatiles were removed under reduced pressure and the crude product was purified by column chromatography (S-X3 resin: crosslinked polystyrene-divinyl benzene 40-80 µm beads, dichloromethane) yielding the [2]rotaxane as a pale-yellow solid (34%; the product was obtained as a mixture of protonated and non-protonated species after column chromatography). ^{1}H NMR (600 MHz, toluene-d_8) δ 7.13-6.93 (m), 6.79-6.65 (m), 4.06 (t), 3.80 (m), 3.69 (s), 3.64 (m), 3.39 (m), 2.18 (m), 2.12 (m), 1.53 (m), 1.50 (m), 1.35-1.17 (m), 0.94 (t) ppm. ^{13}C NMR (101 MHz, $CDCl_3$) δ 179.5, 174.2, 148.1, 145.4, 128.6, 128 (m), 126.2, 125.8, 121.7, 114.4, 71.1, 69.9, 69.5, 64.6, 63.2, 40.6, 34.6, 34.2, 32.1, 29.9-29.8 (m), 26.1, 25.9, 25.2, 24.9, 22.8, 14.3 ppm. MALDI-ToF-MS: found 1151.607 m/z (clcd. 1151.419 m/z for M); 1137.643 m/z (clcd. 1137.481 m/z for [M-S]+NH_4^+). HR-ESI MS: 1136.4502 m/z (clcd. 1136.4734 m/z for [M-SH]+NH_4^+)

2. Supplementary information for out-of-equilibrium experiments

2.1. Dissipative activation and switching of optical behavior of fluorophores

Fueling with a small molecule

To confirm the cascaded fluorophore activation by the linear propagation of molecular signals through spectroscopic investigations using propane thiol as a model fuel (Supplementary Fig. 1a), a solution of acridinium perchlorate (12 mM) and the naphthalimide fluorophore (OFF-state, 12 mM) in DMSO-d_6 (1 mL) was prepared. With half of the solution (0.5 mL), a ^{1}H NMR spectrum was recorded (initial state, OFF, Supplementary Fig. 1b, lower spectrum) and afterwards propane thiol (6 eq.) was added. After 30 min, a ^{1}H NMR spectrum was recorded (activated state, ON, Supplementary Fig. 1b, upper spectrum). The characteristic peak at ca. 5.4 ppm indicates the Thiol-Michael reaction between acridinium perchlorate and propane thiol.

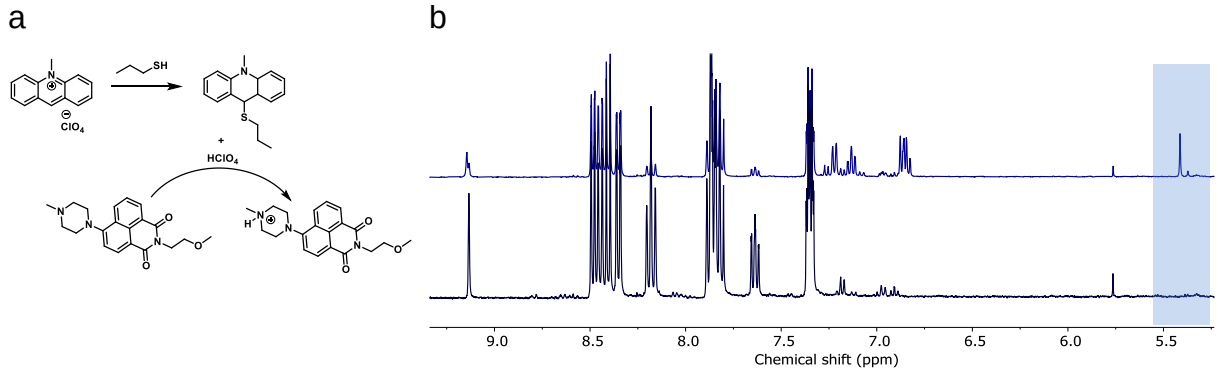

Supplementary Figure 1: Cascaded fluorophore activation with a model fuel. a, Reaction scheme of fueling reaction with propane thiol. b, Stack of ^{1}H NMR spectra of the reaction mixture containing acridinium perchlorate and the naphthalimide fluorophore in DMSO-d_6 before (lower spectrum) and after the addition of propane thiol (upper spectrum), displaying the occurrence of a distinct signal (highlighted in blue).

The other half (0.5 mL) of the OFF state solution was diluted to a final concentration of 0.2 mM of acridinium perchlorate and naphthalimide fluorophore, and a fluorescence spectrum was recorded (OFF state). Afterwards, 6 eq. of propane thiol were added and a fluorescence spectrum was recorded after 30 min (ON state, Supplementary Fig. 2).

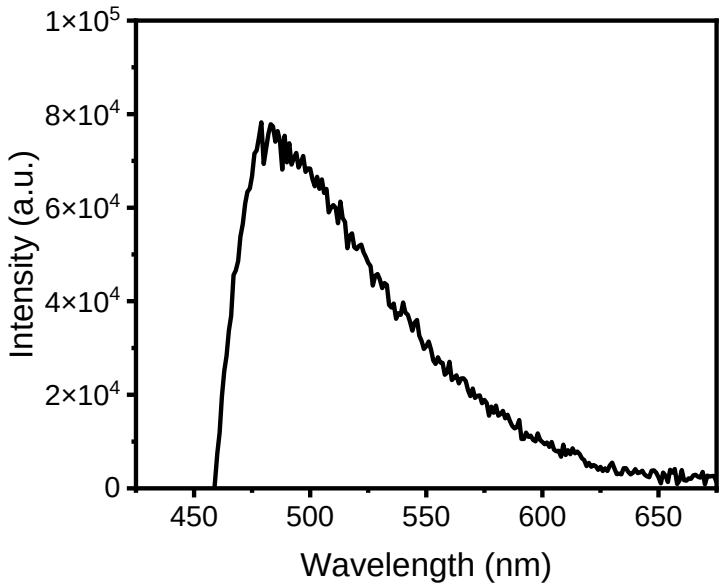

Supplementary Figure 2: Fluorescence spectrum of the reaction mixture containing the acridinium perchlorate and the naphthalimide fluorophore after the addition of propane thiol, recorded at an excitation wavelength of 360 nm. Background fluorescence from the initial state was subtracted.

Ultrasound-induced dissipative activation of naphthalimide fluorophore

All experiments for the US-induced activation of the naphthalimide fluorophore were performed at concentrations of 4.0 μM of fluorophore and molecular switch, and 6.0 μM of polymer (see Methods for sonication details). All spectra were recorded after a 30 min equilibration period. To verify thiol formation after 10 min ultrasonication, the scission product was incubated with a thiol-selective probe. After 2 d incubation, an increase in fluorescence of the released dansyl fluorophore was observed, proving thiol formation (Supplementary Fig. 3).

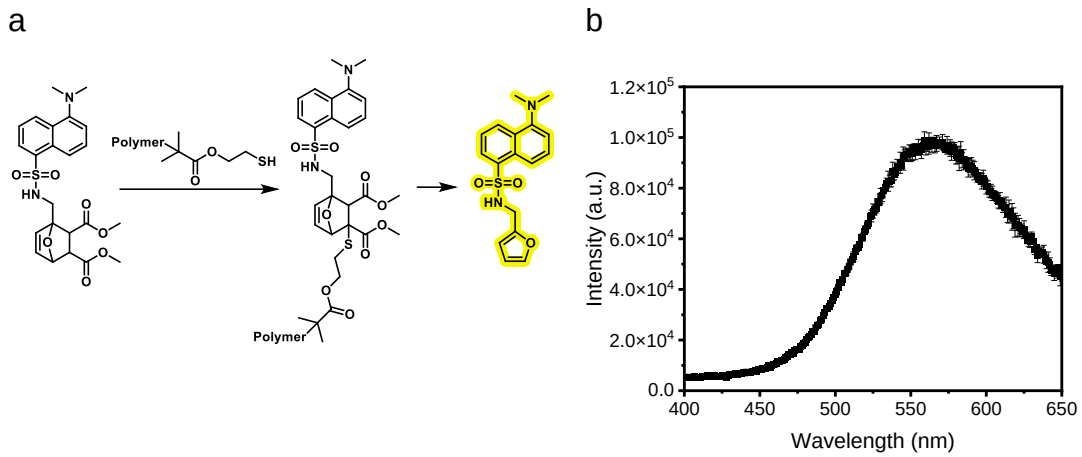

Supplementary Figure 3: Observation of thiol formation by thiol-selective probe. a, Reaction scheme of the addition of the generated thiol to the thiol-selective probe and subsequent dansyl fluorophore release. b, Increase in fluorescence intensity of the dansyl fluorophore, recorded at an excitation wavelength of 360 nm.

As a control experiment, to exclude any direct influence of US on the fluorophore, a pre-sonicated polymer sample (ex-situ) was added to the reaction mixture containing the acridinium perchlorate and the fluorophore. The resulting fluorescence emission intensity was in the same order of magnitude (10^6 a.u.) compared to the in-situ sonicated samples (Supplementary Fig. 4). This confirms the mechanochemically-induced fueling rather than a direct effect of US (see also Supplementary Fig. 9 for an additional control). As control experiment to exclude unspecific activation of the polymer, the acridinium perchlorate, the naphthalimide fluorophore, and the polymer were mixed, but not exposed to US (Supplementary Fig. 5). The corresponding fluorescence spectrum shows no significant difference to the background without the polymer, demonstrating the necessity of US to release the thiol functionalities.

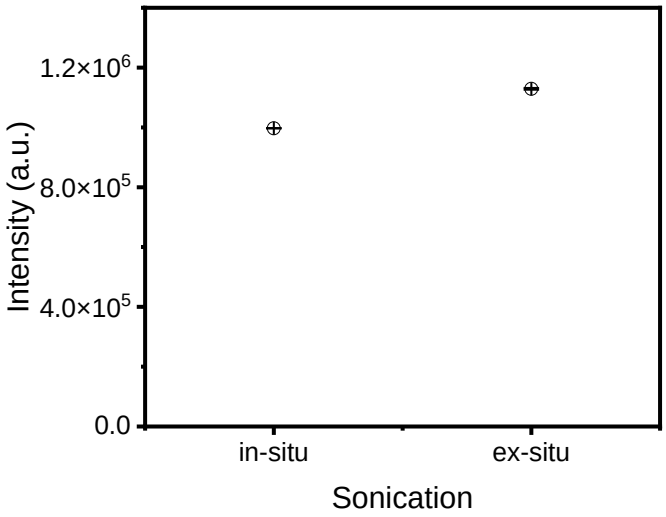

Supplementary Figure 4: Comparison of the maximum intensity of the naphthalimide fluorophore emission at 460 nm for in-situ and ex-situ sonication (ON state), recorded at an excitation wavelength of 360 nm. Background fluorescence from the initial state was subtracted. Error bars represent standard deviations derived from three independent experiments.

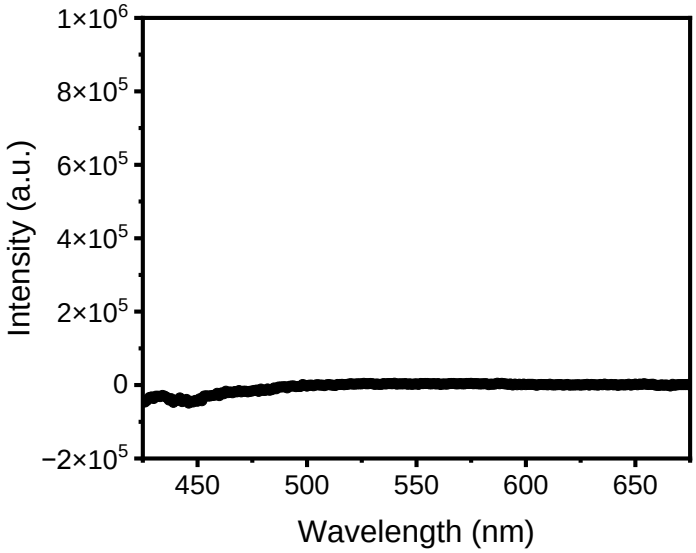

Supplementary Figure 5: Fluorescence spectrum of the reaction mixture containing the acridinium perchlorate, the naphthalimide fluorophore, and the non-sonicated polymer, recorded at an excitation wavelength of 360 nm. Background fluorescence from the initial state was subtracted.

To investigate the dissipation characteristics of the system, two bases with different pK_a values were added in varying amounts to the ON state of the reaction mixture. First, the equivalents of 1,5,7-triazabicyclo[4.4.0]dec-5-ene (TBD, pK_a = 26.0 in acetonitrile) were varied (Supplementary Fig. 6) and 0.5 eq. were chosen as the base concentration for further experiments.

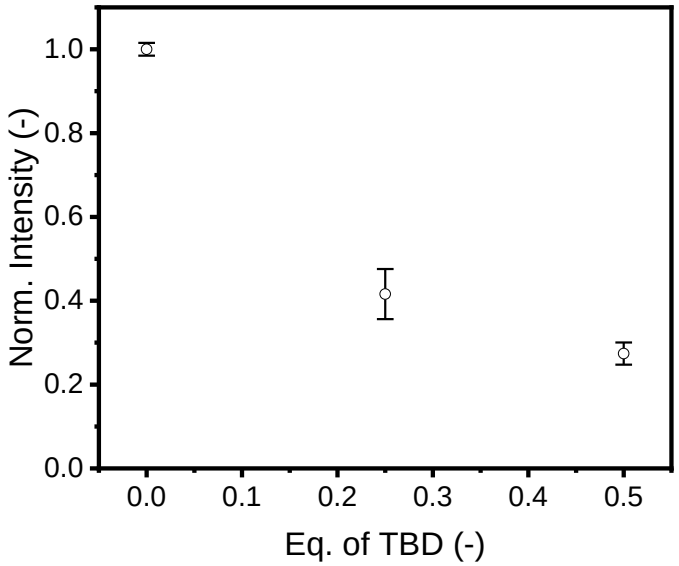

Supplementary Figure 6: Normalized maximum fluorescence emission intensity of the naphthalimide fluorophore (ON state) in presence of 0-0.5 eq. of TBD as base, recorded at an excitation wavelength of 360 nm. Background fluorescence from the initial state was subtracted. Error bars represent standard deviations derived from three independent experiments.

Second, a significantly weaker base, *i.e.*, triethylamine (NEt_3, pK_a = 10.8) was added to the ON state and only a very small decrease of the fluorescence emission (< 10%) was observed (Supplementary Fig. 7). Thus, it was concluded that the basicity of the base is an important parameter to control the dissipation characteristics.

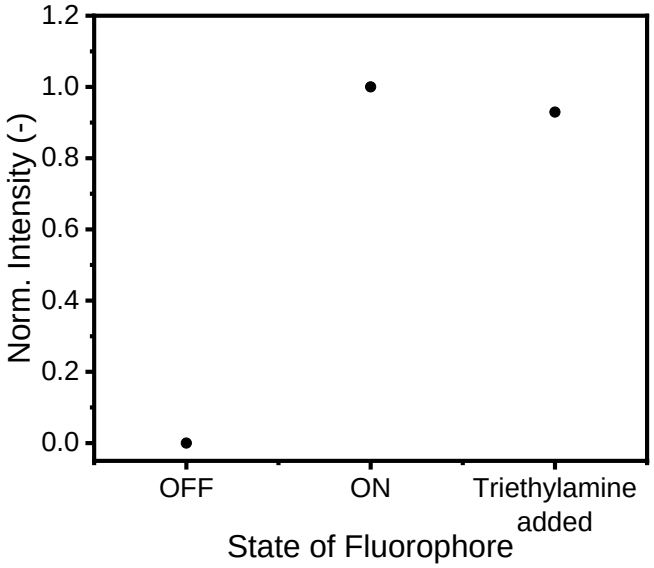

Supplementary Figure 7: Comparison of the normalized maximum fluorescence emission intensity at 460 nm of the naphthalimide fluorophore for the initial state (OFF), the activated state (ON), and in presence of 0.5 eq. triethylamine as a base, recorded at an excitation wavelength of 360 nm. Background fluorescence from the initial state was subtracted.

Further, the US-induced dissipative activation of the naphthalimide fluorophore was tested in a turbid environment, in which light cannot operate. For this, silica was added to the reaction mixture before sonication to create a turbid mixture. Additionally, a large excess of rhodamine B was added to create a colored solution and demonstrate the ability of US to activate the fueling process under these conditions (Supplementary Fig. 8). The naphthalimide fluorophore could be dissipatively activated in a selective manner in turbid medium in presence of another dye.

a

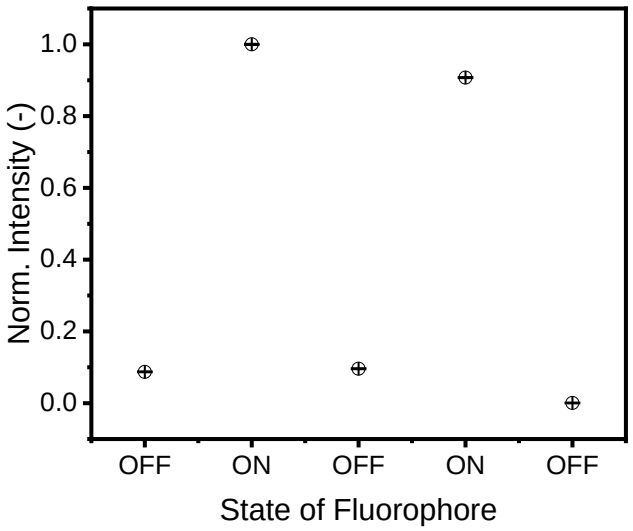

b

Supplementary Figure 8: a, Comparison of the naphthalimide fluorophore emission intensity at 460 nm for the initial state (OFF), the activated states (ON), and the deactivated states (OFF) of a turbid and colored reaction mixture with a large excess of rhodamine B added, recorded at an excitation wavelength of 360 nm. The rhodamine B was filtered before recording fluorescence spectra, and the remaining dye did not interfere with the recording of the naphthalimide spectra due to distinctly different excitation and fluorescence characteristics. b, Photograph of the sonication process of the sample. Error bars represent standard deviation derived from two independent experiments.

Mechanodissipative switching of optical behavior of perylene-based NIR emitters

In addition to the fluorescence excitation maximum at ca. 380 nm, the excitation spectrum of the PMI primary amine also exhibits a second maximum at ca. 520 nm, which is altered upon activation or deactivation of the reaction network (Supplementary Fig. 9).

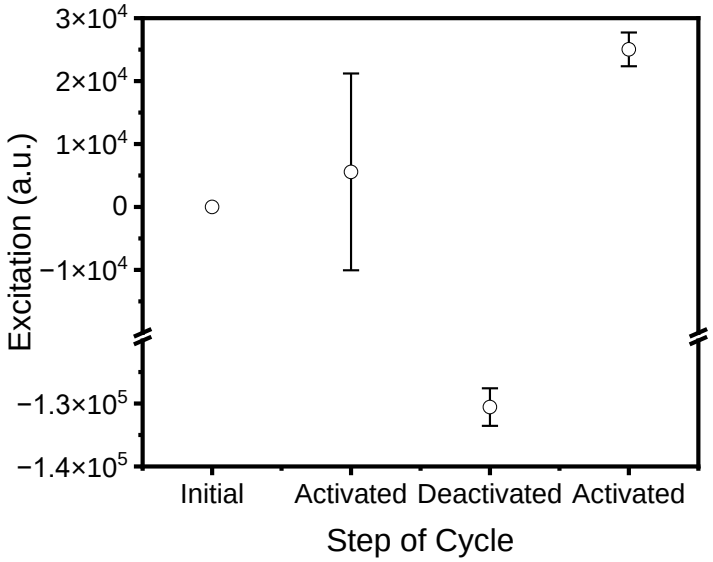

Supplementary Figure 9: Mechanochemically fueled activation of the low-wavelength excitation state (524 nm) of 1° PMI amine recorded at 590 nm emission wavelength. Background fluorescence from the initial state was subtracted. Error bars represent standard deviation derived from independent experiments.

2.2. Transient macrocycle positioning in and dissipative catalysis with a [2]rotaxane

As an additional control experiment to exclude any direct effect of the US on the functional molecule (e.g., destruction of the functional molecule or interaction of sonotrode impurities with the amine functionality), the reaction mixture without polymer was subjected to US. This control experiment was performed for the [2]rotaxane since it is the largest of the functional molecules and thus would be most susceptible to US. Two independent sonication experiments were performed in analogy to the experiments with polymer, and no increase in fluorescence emission intensity was observed, proving the non-destructive character of US to the [2]rotaxane and the insensitivity of the functional compound to US (Supplementary Fig. 10).

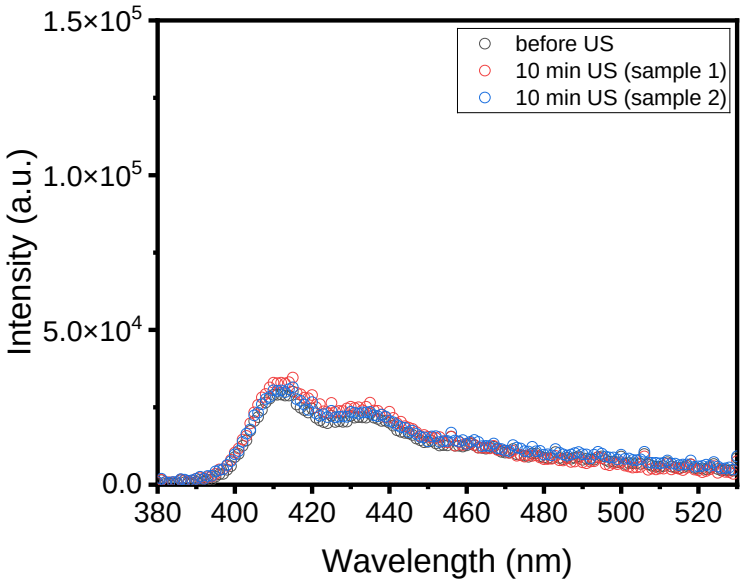

Supplementary Figure 10: Fluorescence emission spectra of the reaction network containing the [2]rotaxane in the initial state (black) and after 10 min US in absence of the polymer (two independent samples, red and blue), recorded at an excitation wavelength of 368 nm.

For the dissipative macrocycle positioning, two different bases (TBD and NEt_3) were tested and both showed consistent behavior (Supplementary Fig. 11). To further study the influence of the base equivalents on the reversion of the ON state to the OFF state, different equivalents of NEt_3 (0-36 eq.) were added to the ON state. The largest influence was observed for adding the first 3 eq. and a saturation behavior was observed for higher amounts of NEt_3 (Supplementary Fig. 12). Consequently, the addition of 0-3 eq. TBD was investigated as well, showing analogous behavior (Supplementary Fig. 13).

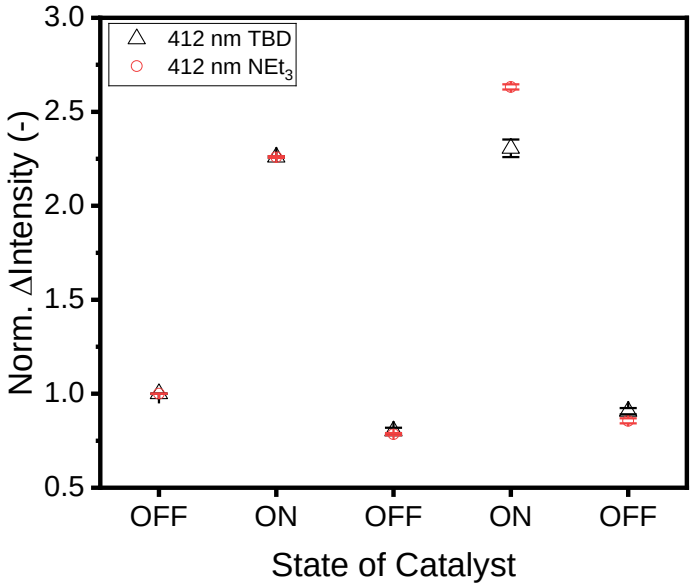

Supplementary Figure 11: Normalized difference in emission intensity obtained at 412 nm showing the switchable positioning of the macrocycle in presence of TBD (black, 3 eq.) or triethylamine (red, 36 eq.) as a base. The fluorescence emission data were obtained after subjecting the reaction mixture to ultrasound for 10 min, recorded at an excitation wavelength of 368 nm. Error bars represent standard deviations derived from three independent experiments.

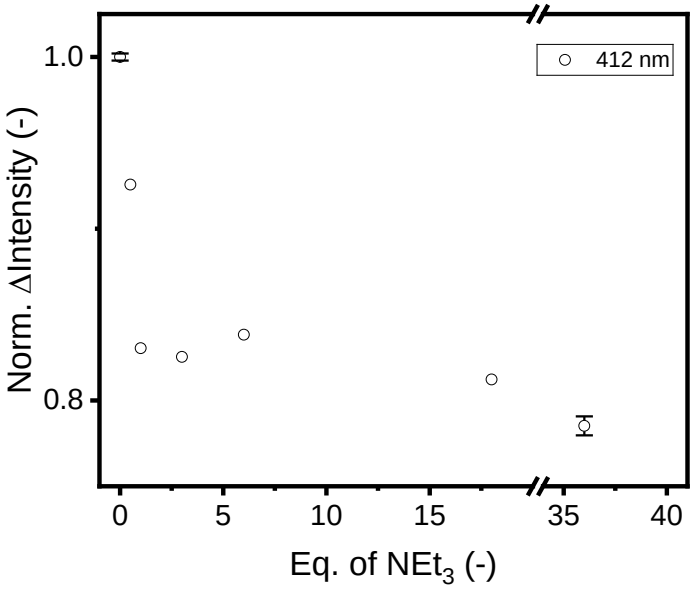

Supplementary Figure 12: Normalized difference in emission intensity obtained at 412 nm showing the switchable positioning of the macrocycle in presence of triethylamine as a base (0-36 eq.). The fluorescence emission data were obtained after subjecting the reaction mixture to ultrasound for 10 min, recorded at an excitation wavelength of 368 nm. Error bars for 0 and 36 eq. NEt_3 represent standard deviations derived from three independent experiments.

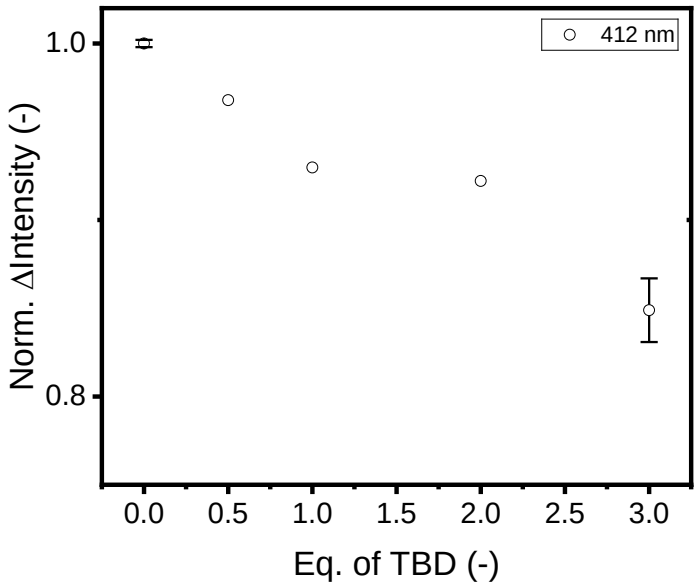

Supplementary Figure 13: Normalized difference in emission intensity obtained at 412 nm showing the switchable positioning of the macrocycle in presence of TBD as a base (0-3 eq.). The fluorescence emission data were obtained after subjecting the reaction mixture to ultrasound for 10 min, recorded at an excitation wavelength of 368 nm. Error bars for 0 and 3 eq. TBD represent standard deviations derived from three independent experiments.

To investigate the dissipative catalytic performance of the [2]rotaxane, first the background reaction rate was determined (Supplementary Fig. 14). Here, data points were merged from three independent experiments.

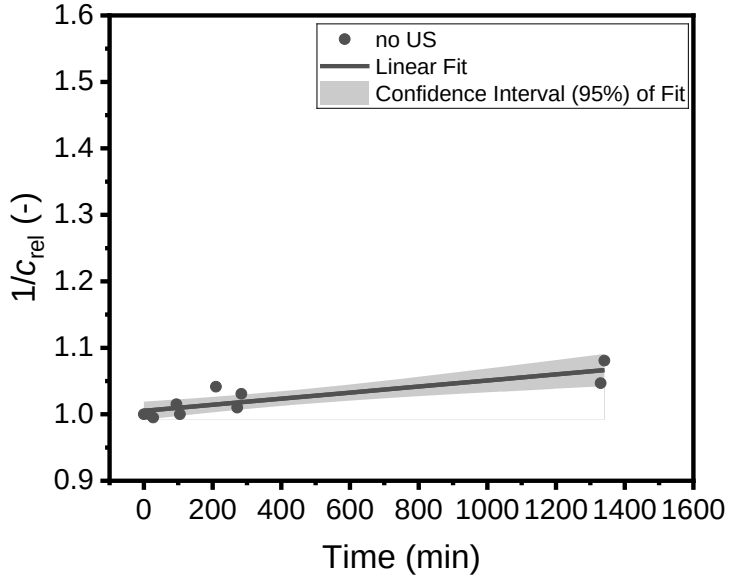

Supplementary Figure 14: Reaction between nitrostyrene and Hantzsch ester in presence of the acridinium perchlorate, the [2]rotaxane, and the polymer without sonication, defined as the background reaction. A linear fit (R^2 = 0.74) was applied to determine the rate constant as the slope of the linear fit (k = (4.563 · 10^{-5} ± 0.966 · 10^{-5}) min^{-1}).

Afterwards, the reaction rate after US exposure was determined applying a linear fit covering the first 400 min after activation of the system (Supplementary Fig. 15), to account for the catalyst deactivation over time (as observed by NMR, Fig. 5). Here, data points were merged from N = 3 independent experiments. All measured ^{1}H NMR integrals used to determine the kinetic rate constants are displayed in Supplementary Table 1.

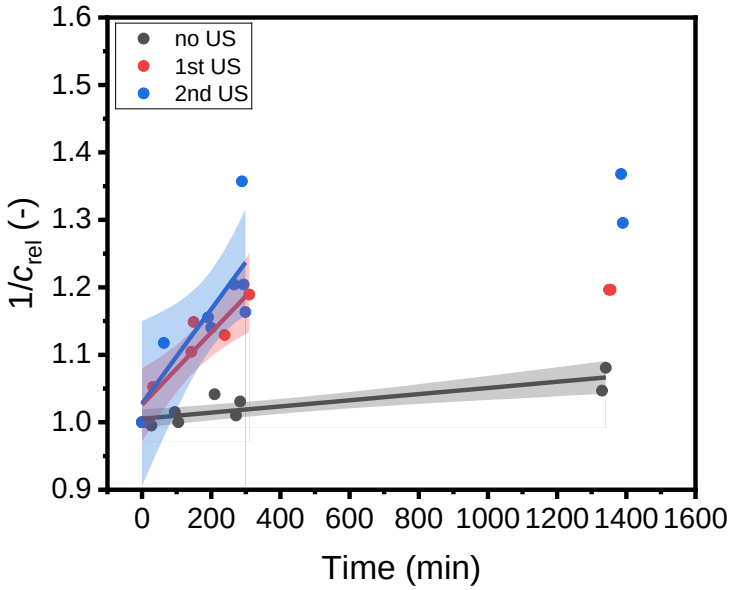

Supplementary Figure 15: Reaction between nitrostyrene and Hantzsch ester in presence of the acridinium perchlorate, the [2]rotaxane, and the polymer without sonication (black), after first sonication (10 min, red), and after second sonication (10 min, blue), with respective linear fits and 95% confidence intervals of the fit.

Supplementary Table 1: NMR integrals of nitrostyrene double bond signal, measured against internal reference (TMS).

Reaction time (min)	w/o US	1st US exposure	2nd US exposure
0	2.01	2.01	1.71
16	2.01		
27	2.02		
32		1.91	
63			1.53
95	1.98		
105	2.01		
143		1.82	
149		1.75	
191			1.48
200			1.50
210	1.93		
239		1.78	
266			1.42
272	1.99		
284	1.95		
289			1.26
294			1.42
299			1.47
310		1.69	
1330	1.92		
1341	1.86		
1350		1.68	
1355		1.68	
1385			1.25
1390			1.32

3. Characterization figures

3.1. NMR spectra

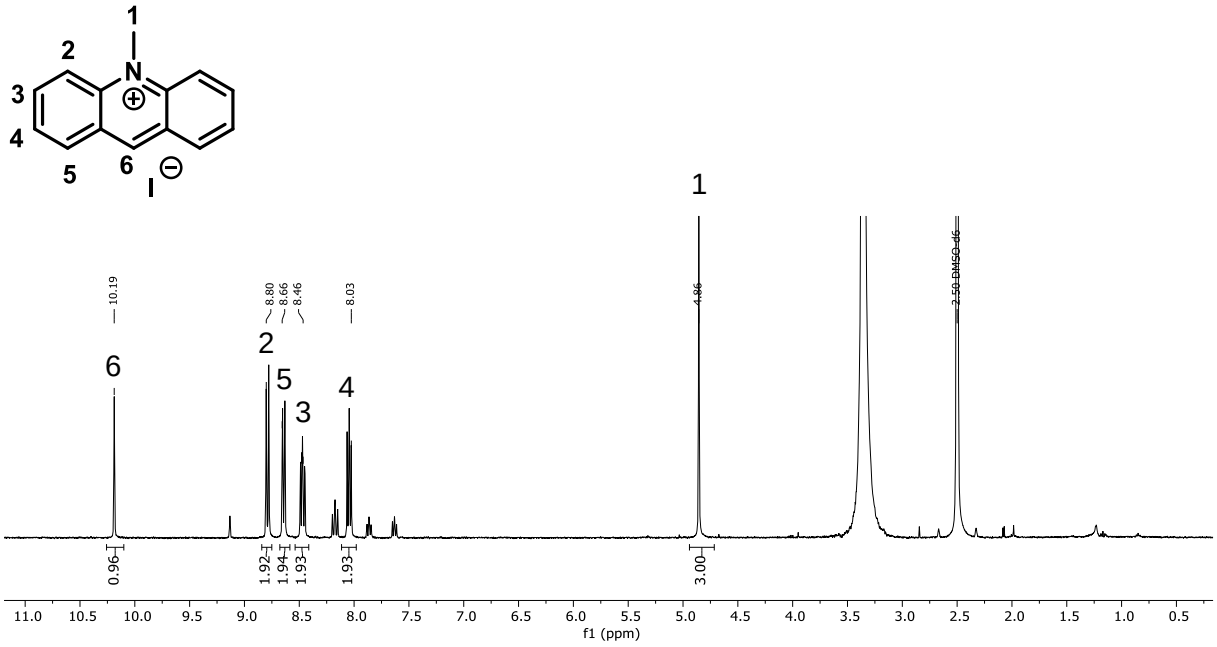

Supplementary Figure 16: ^{1}H NMR spectrum of acridinium iodide in DMSO-d_6.

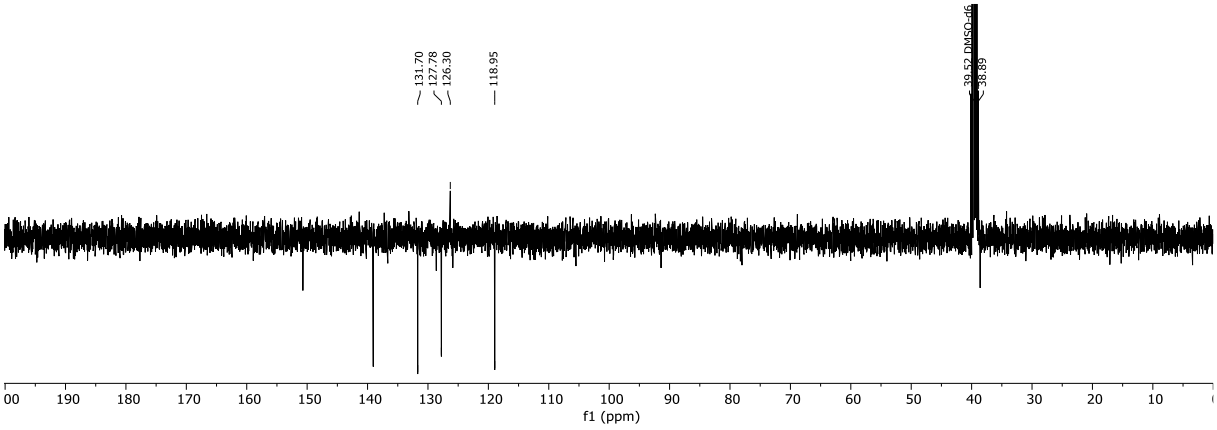

Supplementary Figure 17: ^{13}C NMR spectrum of acridinium iodide in DMSO-d_6.

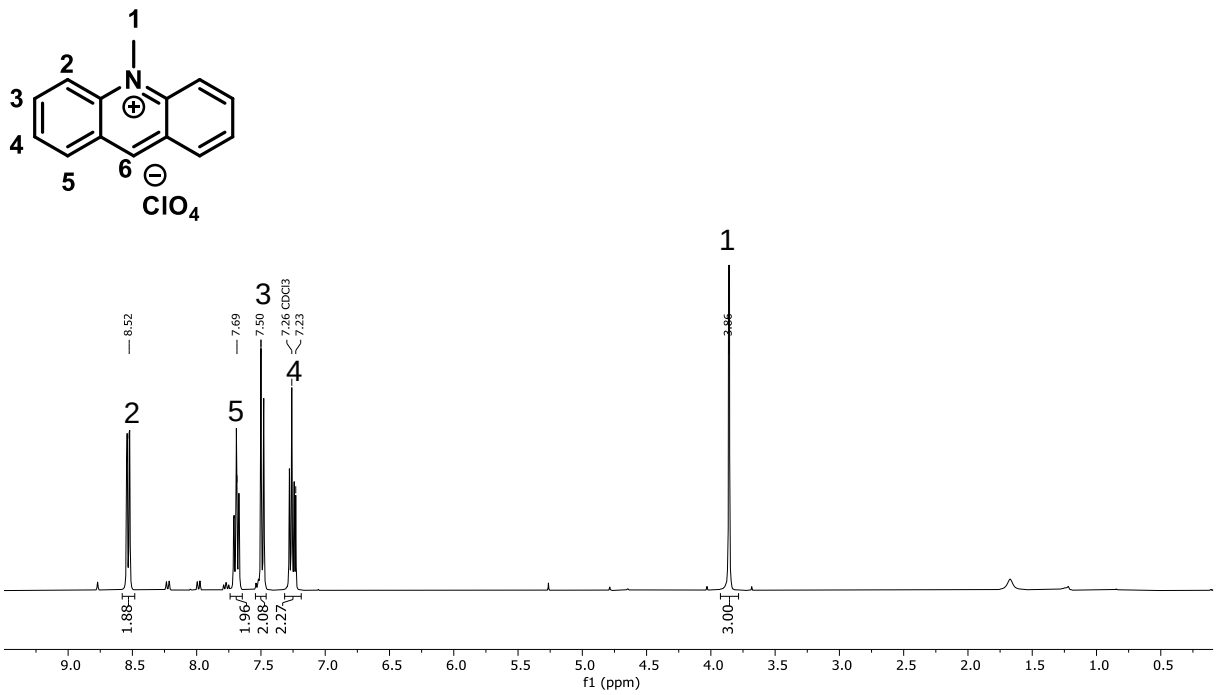

Supplementary Figure 18: ^{1}H NMR spectrum of acridinium perchlorate in $CDCl_3$.

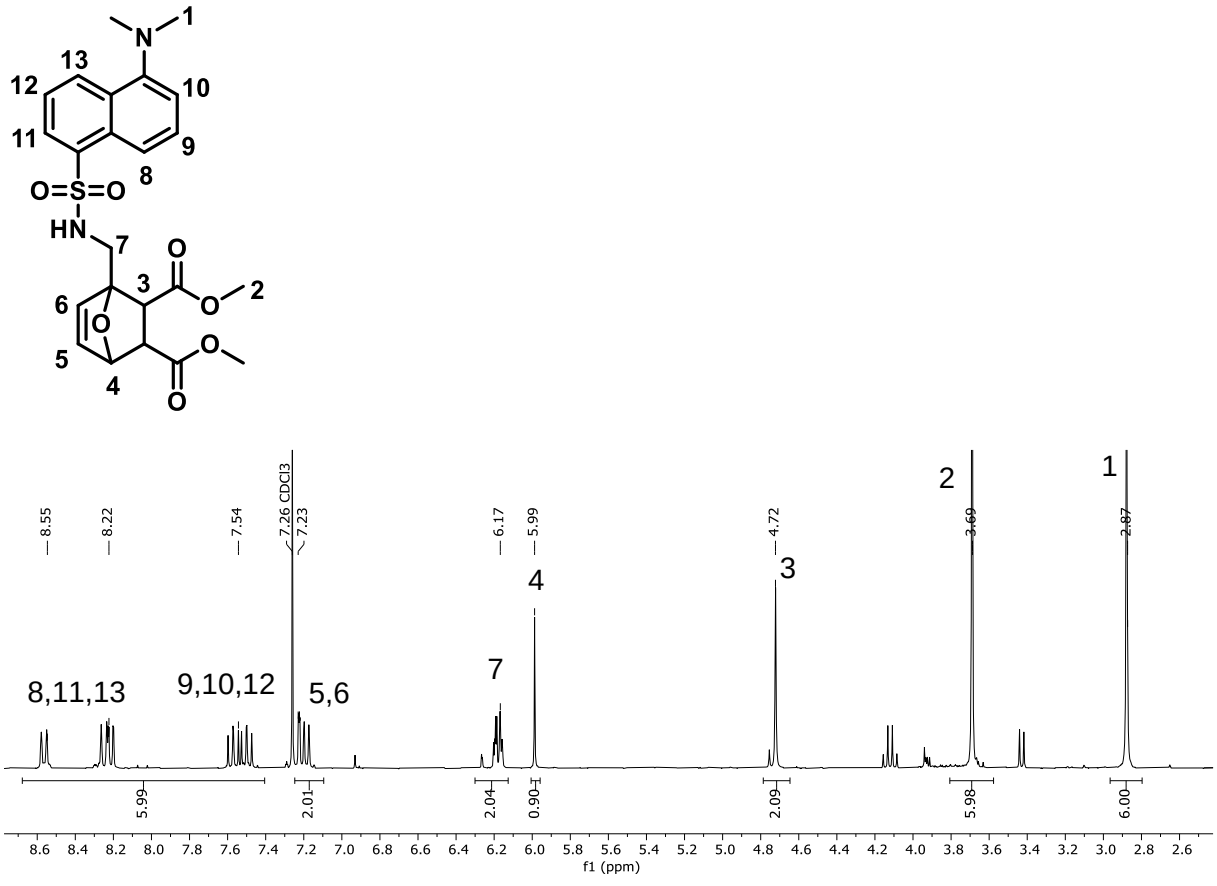

Supplementary Figure 19: ^{1}H NMR spectrum of thiol-selective probe in $CDCl_3$.

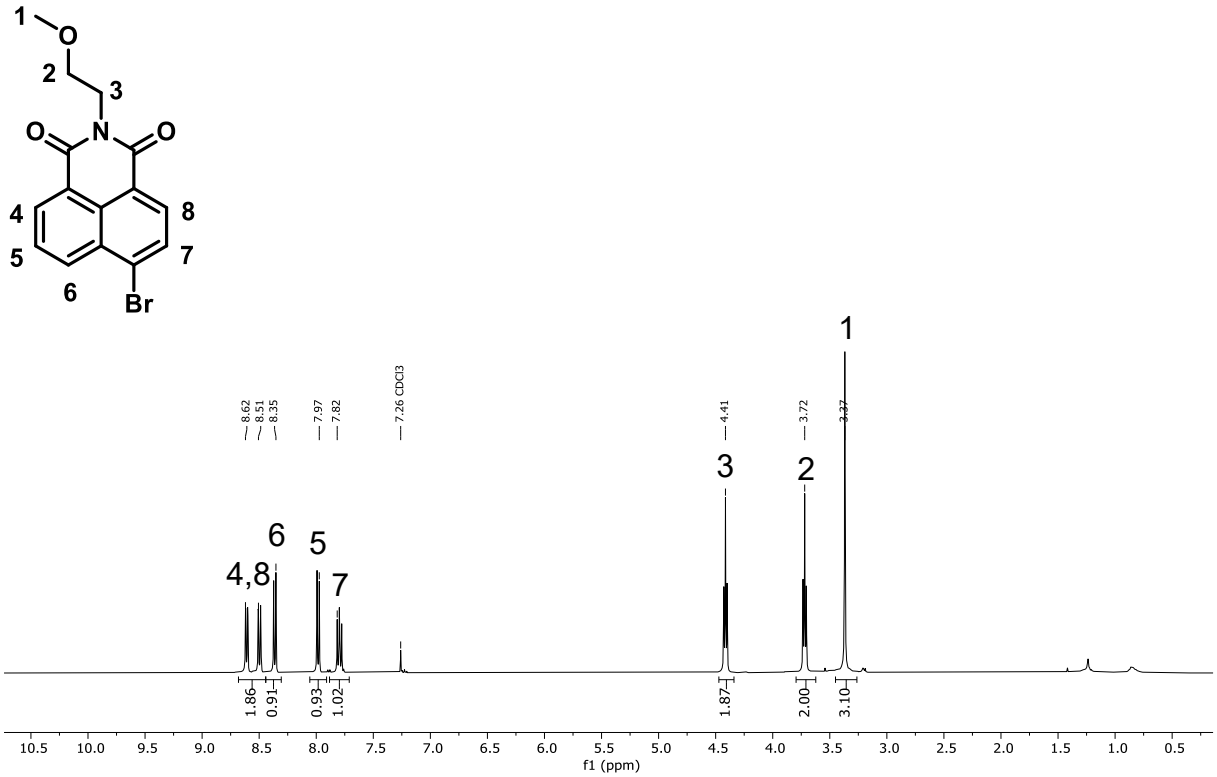

Supplementary Figure 20: ^{1}H NMR spectrum of naphthylic imide-Br in $CDCl_3$.

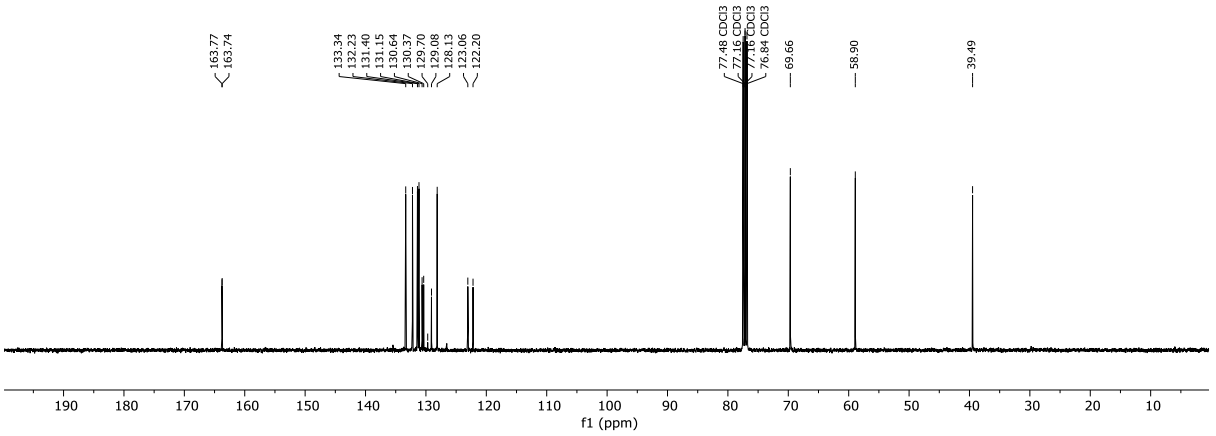

Supplementary Figure 21: ^{13}C NMR spectrum of naphthylic imide-Br in $CDCl_3$.

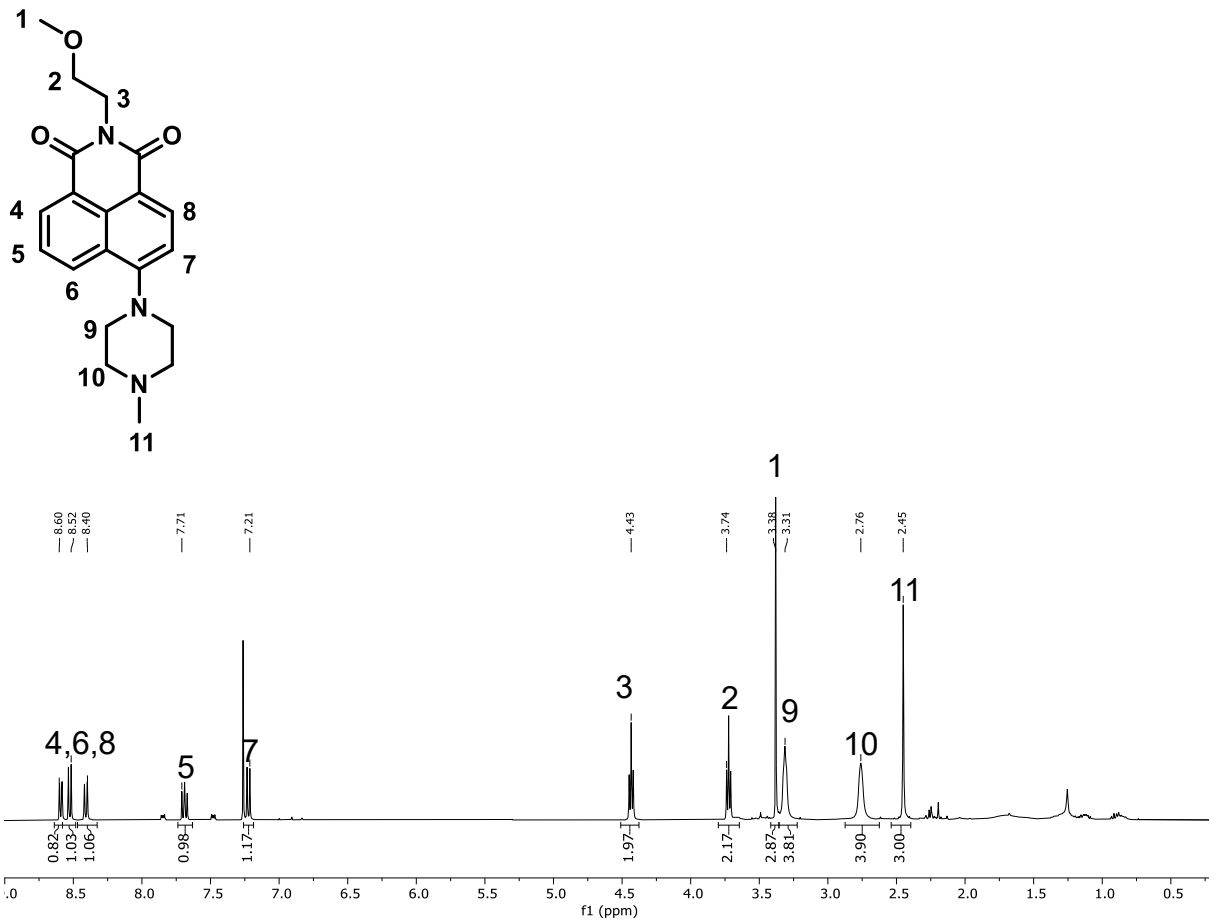

Supplementary Figure 22: ^{1}H NMR spectrum of naphthylic imide amine in $CDCl_3$.

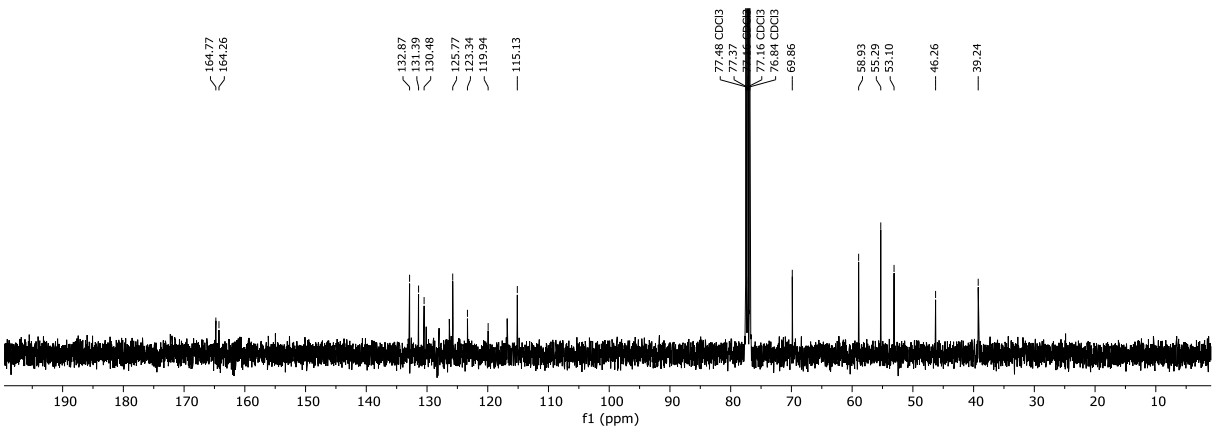

Supplementary Figure 23: ^{13}C NMR spectrum of naphthylic imide amine in $CDCl_3$.

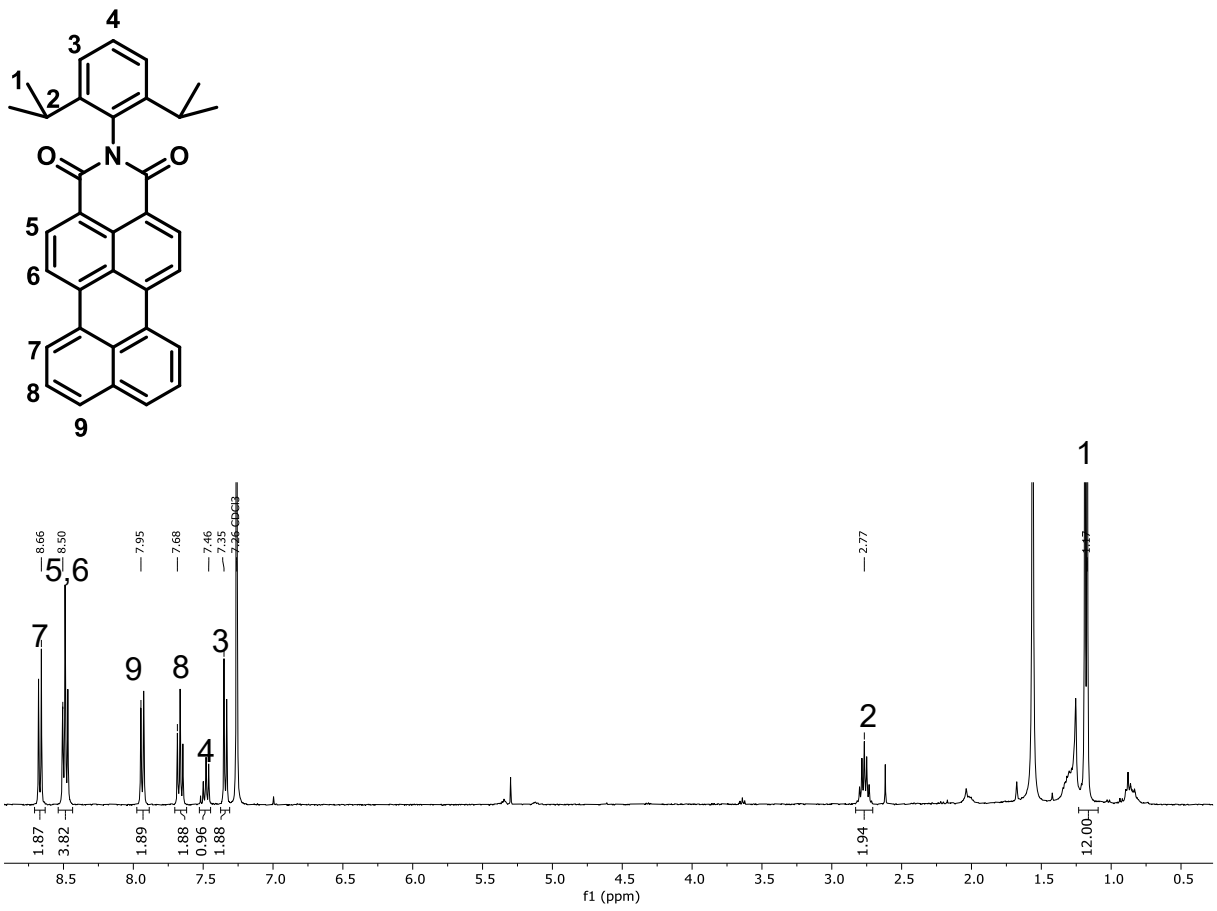

Supplementary Figure 24: ^{1}H NMR spectrum of perylene monoimide in $CDCl_3$.

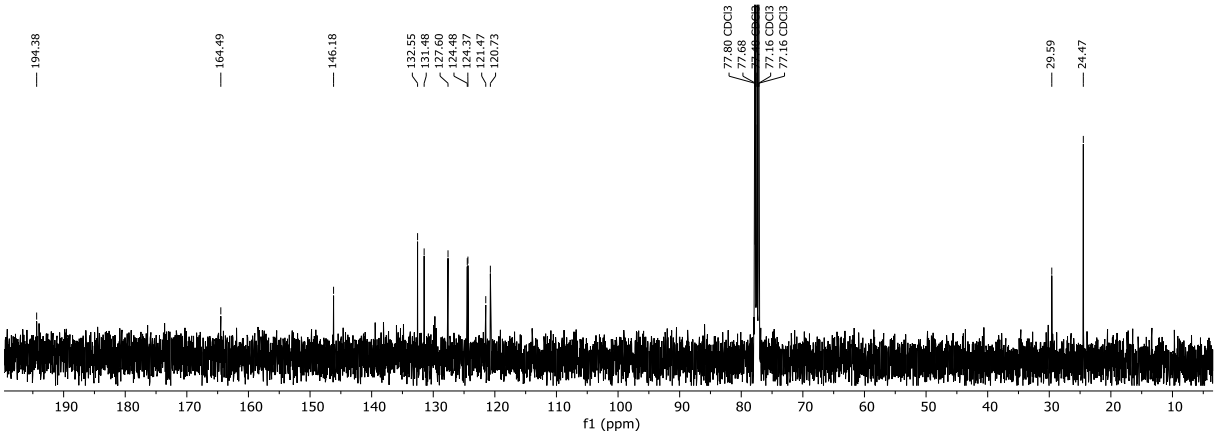

Supplementary Figure 25: ^{13}C NMR spectrum of perylene monoimide in $CDCl_3$.

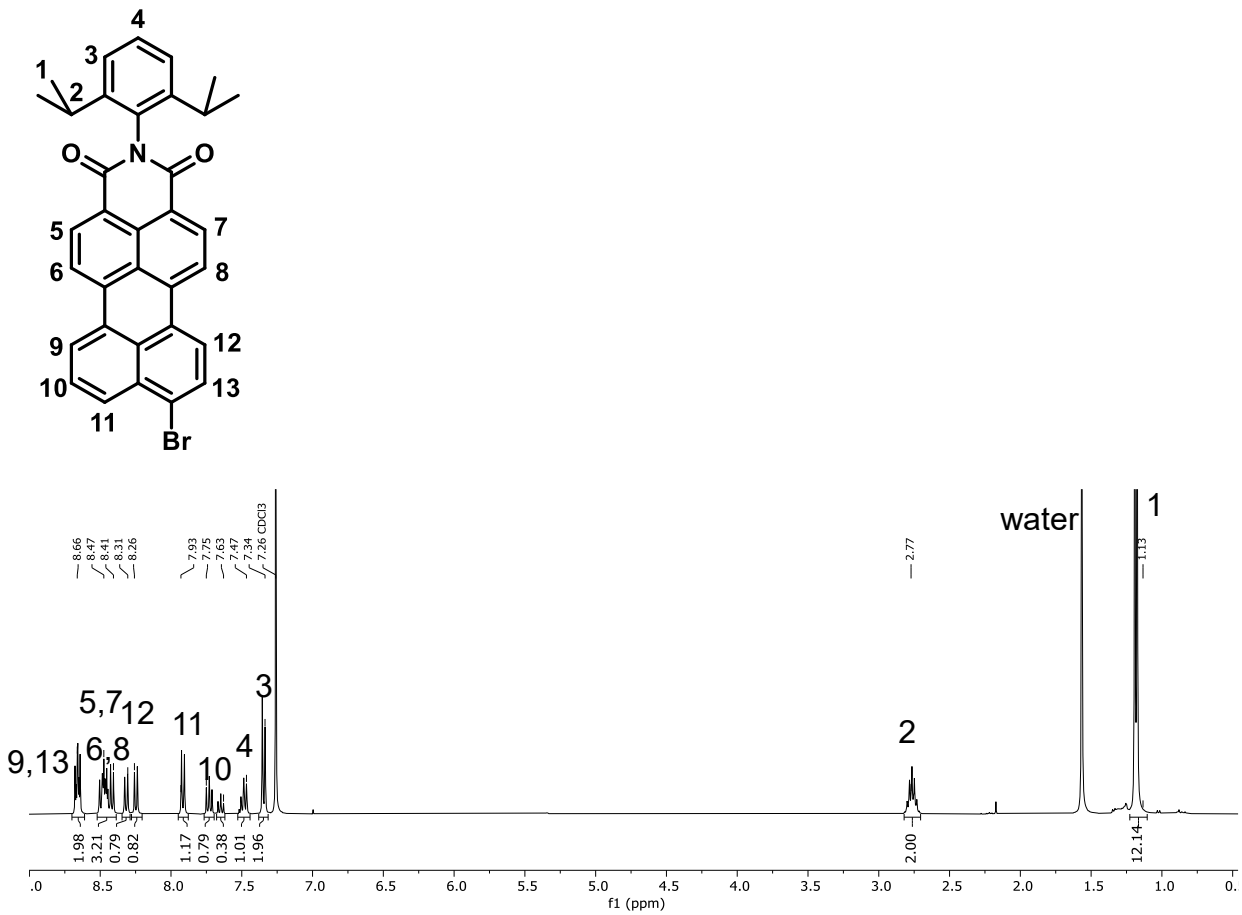

Supplementary Figure 26: ^{1}H NMR spectrum of perylene monoimide bromide in $CDCl_3$.

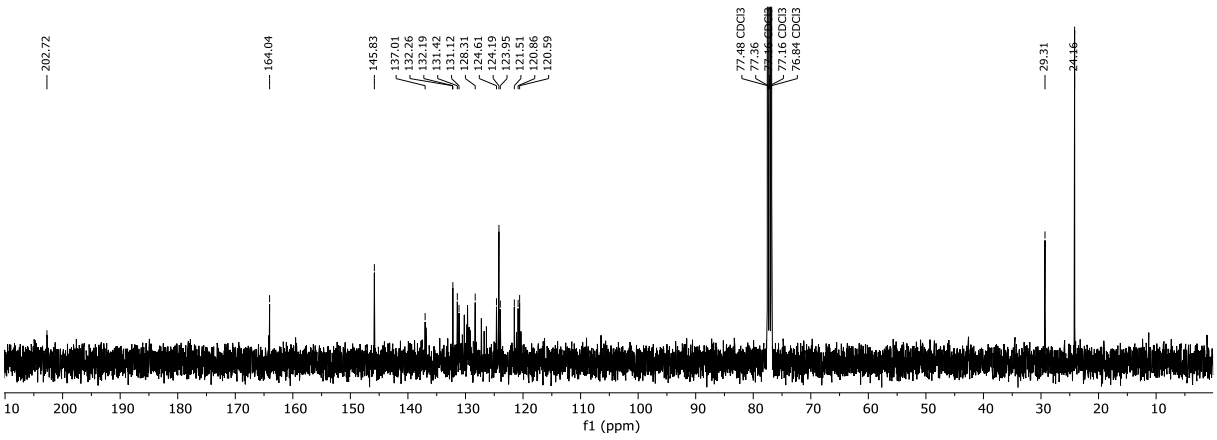

Supplementary Figure 27: ^{13}C NMR spectrum of perylene monoimide bromide in $CDCl_3$.

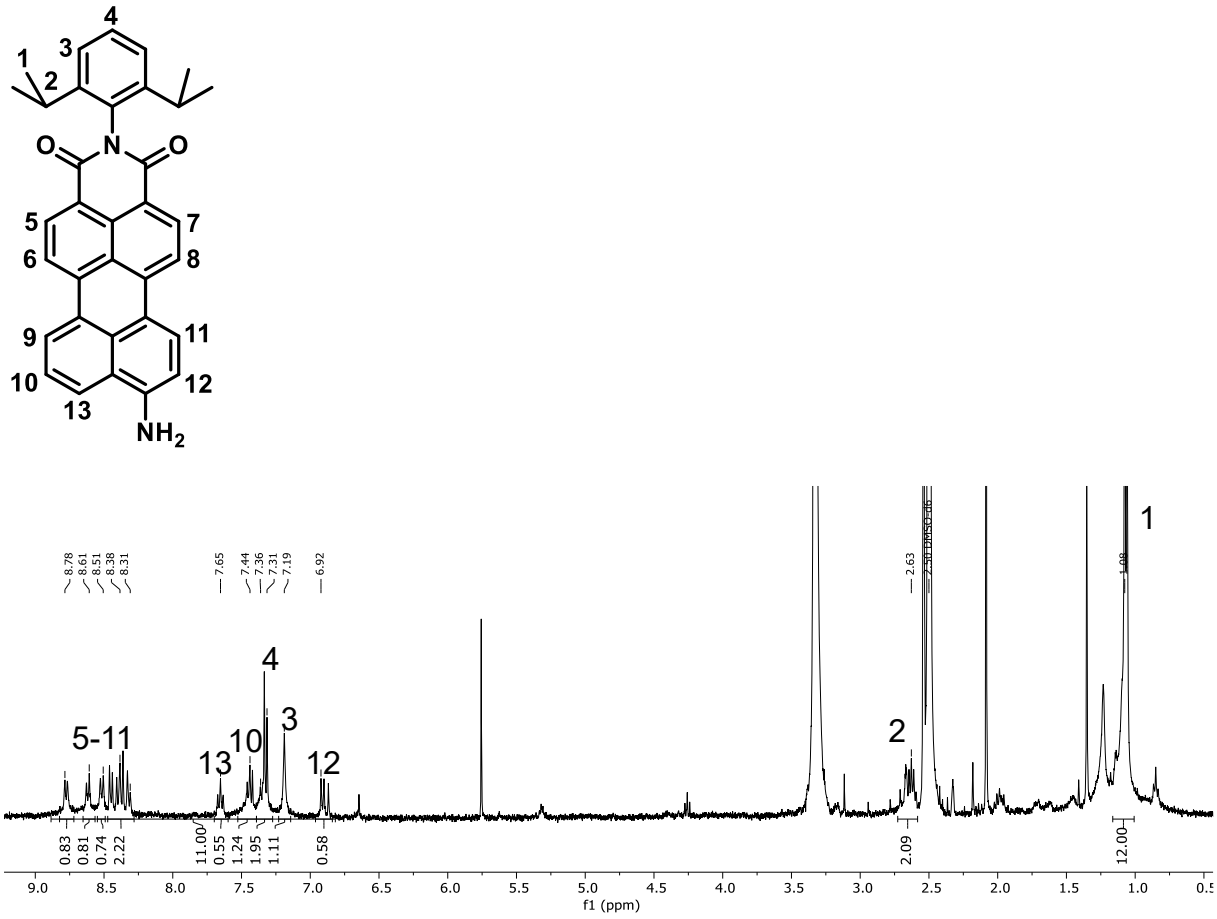

Supplementary Figure 28: ^{1}H NMR spectrum of perylene monoimide primary amine in DMSO-d_6. The low signal intensity was caused by low solubility in common NMR solvents and as reported in literature. Therefore, HR-ESI MS was performed in favor of ^{13}C NMR spectroscopy.

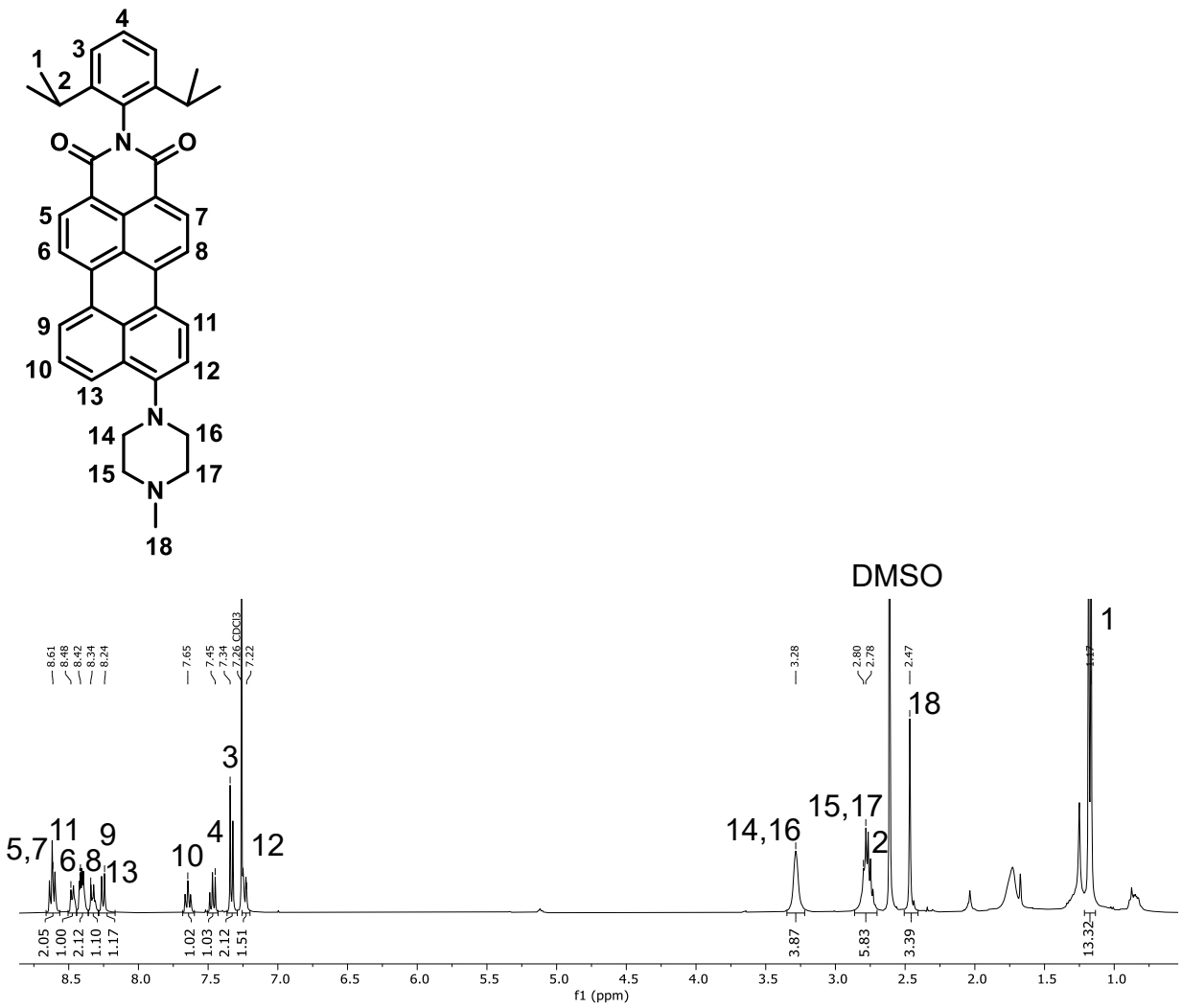

Supplementary Figure 29: ^{1}H NMR spectrum of perylene monoimide tertiary amine in $CDCl_3$.

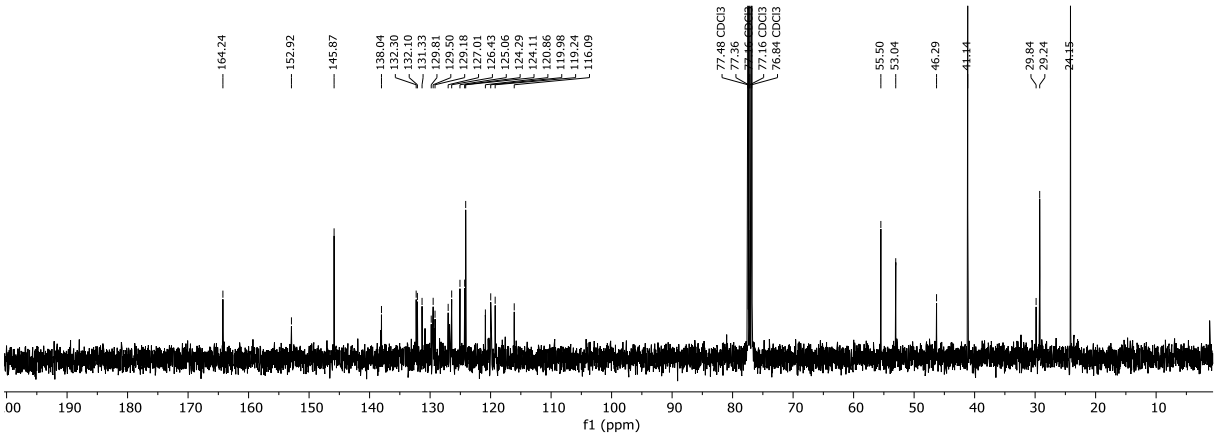

Supplementary Figure 30: ^{13}C NMR spectrum of perylene monoimide tertiary amine in $CDCl_3$.

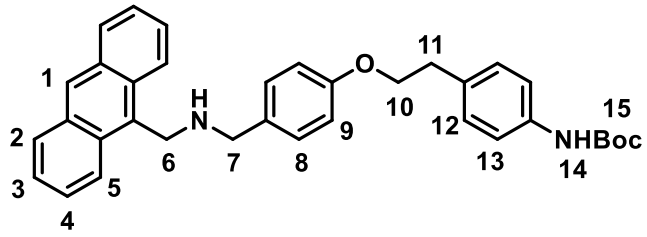

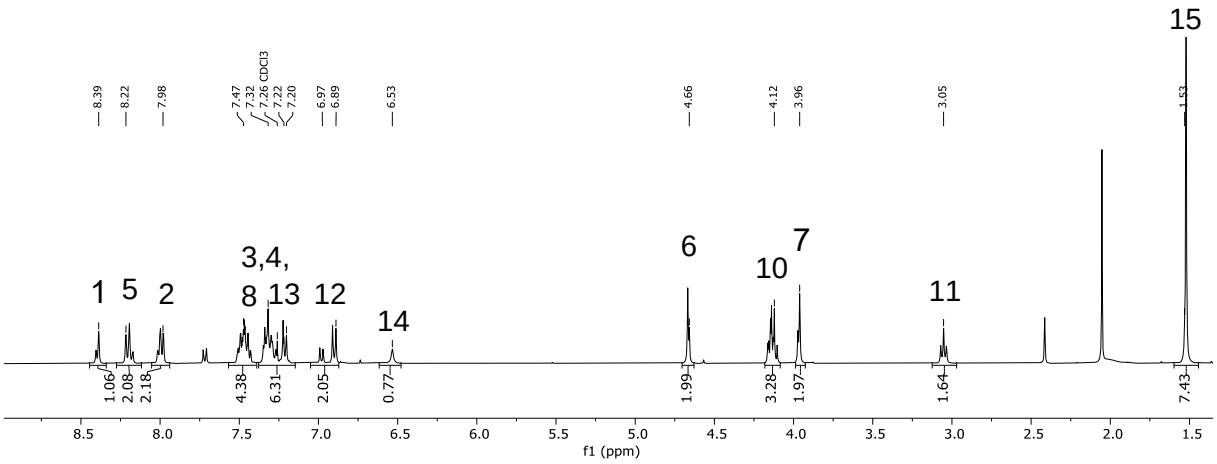

Supplementary Figure 31: ^{1}H NMR spectrum of tert-butyl (4-(2-(4-(((anthracen-9-ylmethyl)amino) methyl)phenoxy)ethyl)phenyl) carbamate in $CDCl_3$.

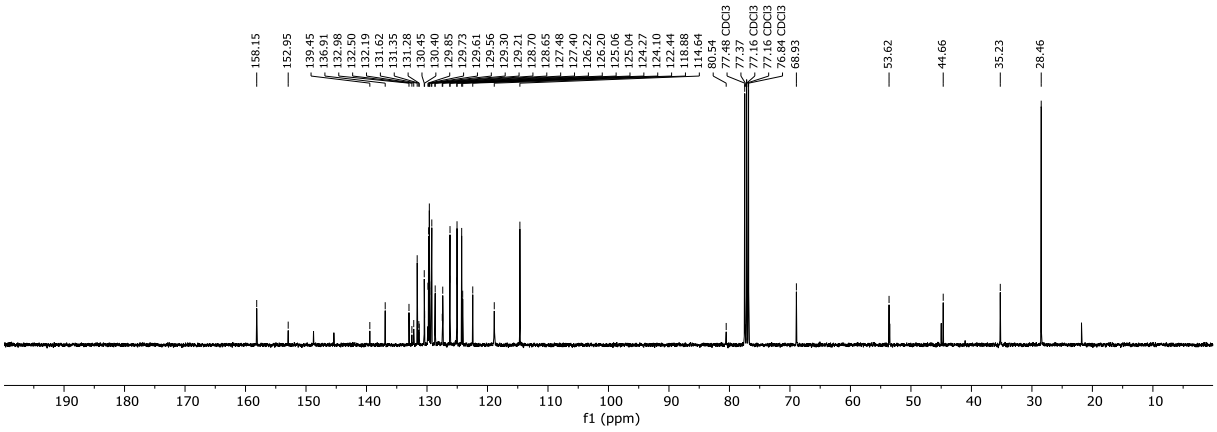

Supplementary Figure 32: ^{13}C NMR spectrum of tert-butyl (4-(2-(4-(((anthracen-9-ylmethyl)amino) methyl)phenoxy)ethyl)phenyl) carbamate in $CDCl_3$.

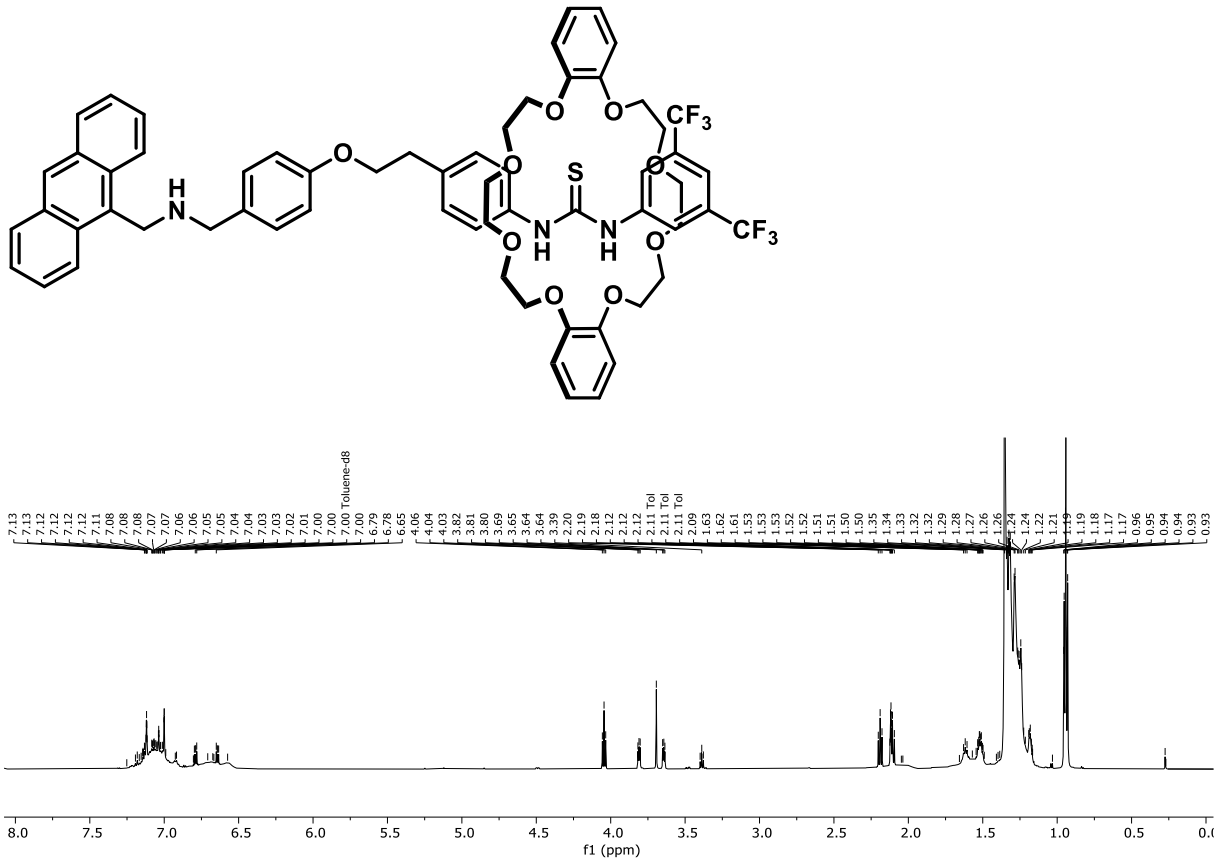

Supplementary Figure 33: ^{1}H NMR spectrum of [2]rotaxane in toluene-d_8.

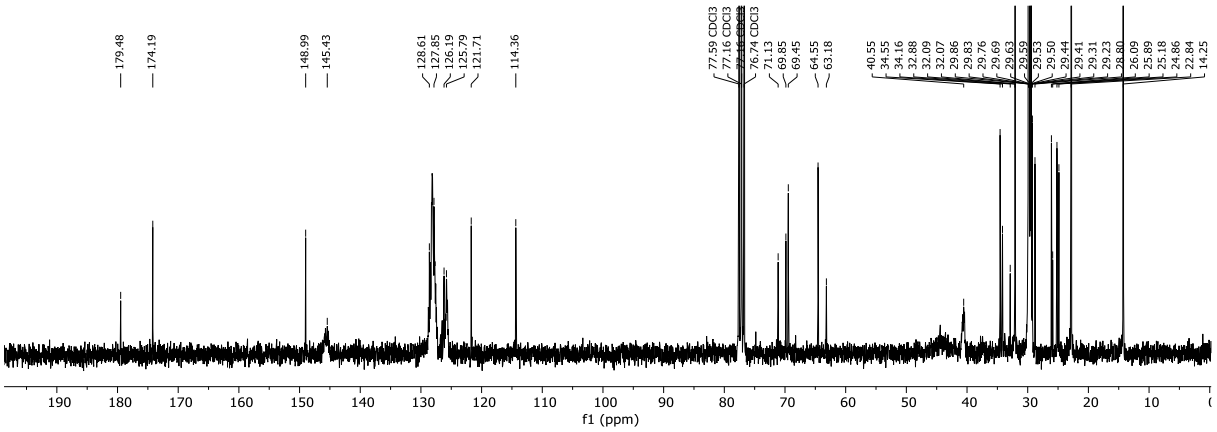

Supplementary Figure 34: ^{13}C NMR spectrum of [2]rotaxane in $CDCl_3$.

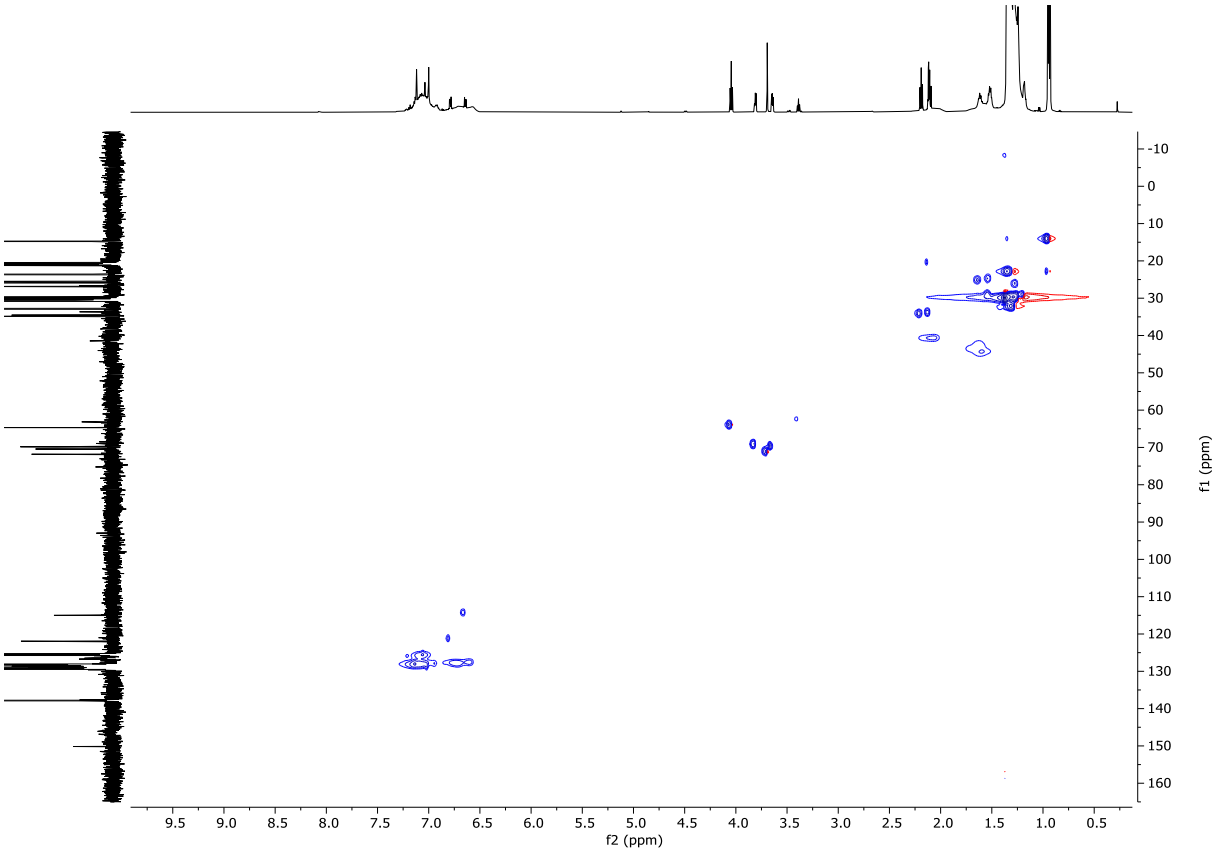

Supplementary Figure 35: ^{1}H ^{13}C HSQC NMR spectrum of [2]rotaxane in toluene-d_8.

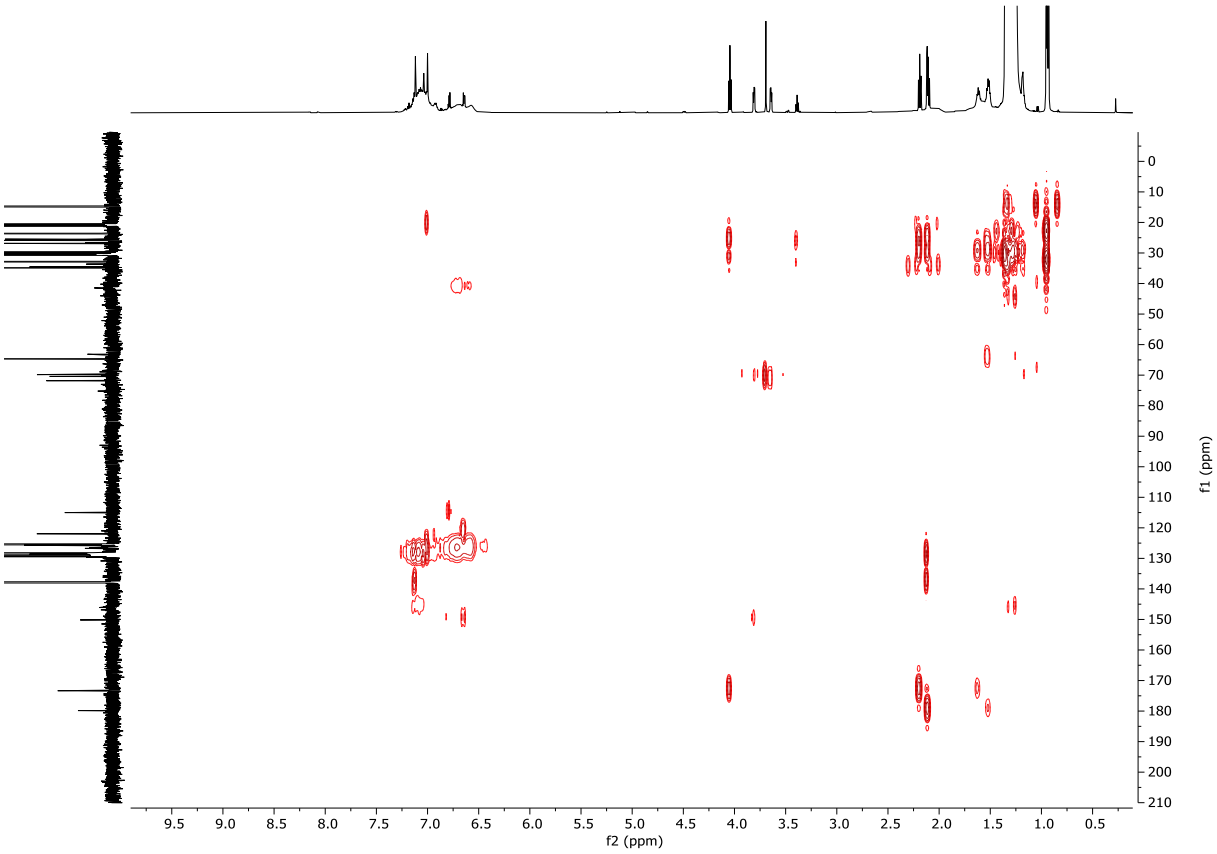

Supplementary Figure 35: ^{1}H ^{13}C HMBC NMR spectrum of [2]rotaxane in toluene-d_8.

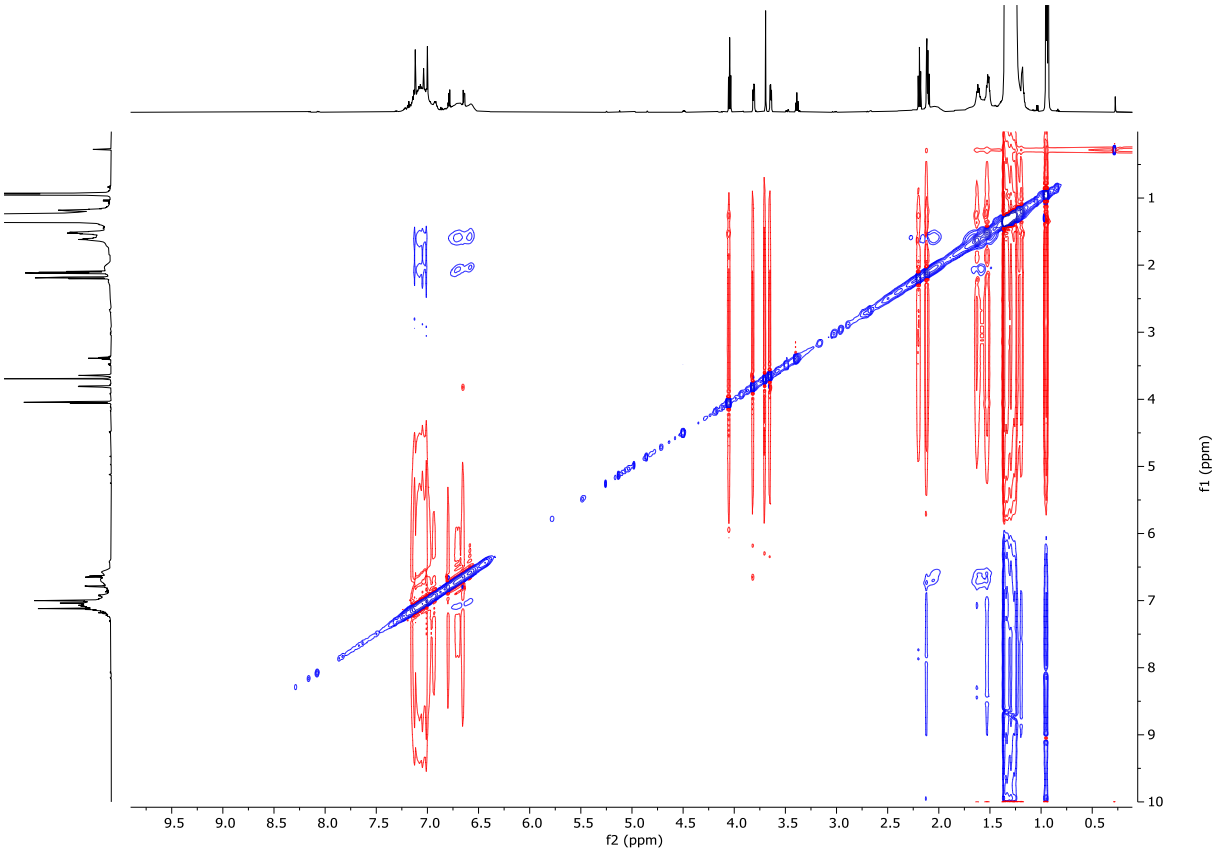

Supplementary Figure 36: ^{1}H ^{1}H NOESY NMR spectrum of [2]rotaxane in toluene-d_8, showing coupling between protons through space.

3.2. High resolution ESI MS and MALDI-ToF MS spectrograms

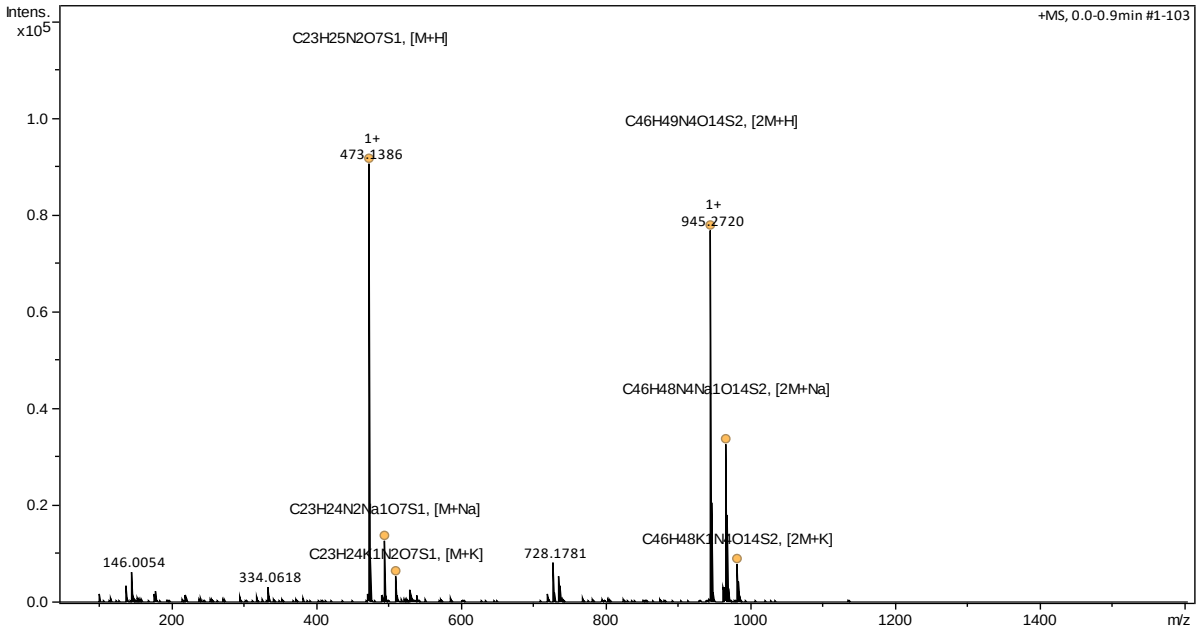

Supplementary Figure 37: HR-ESI MS spectrogram (130-1600 m/z) of thiol-selective probe.

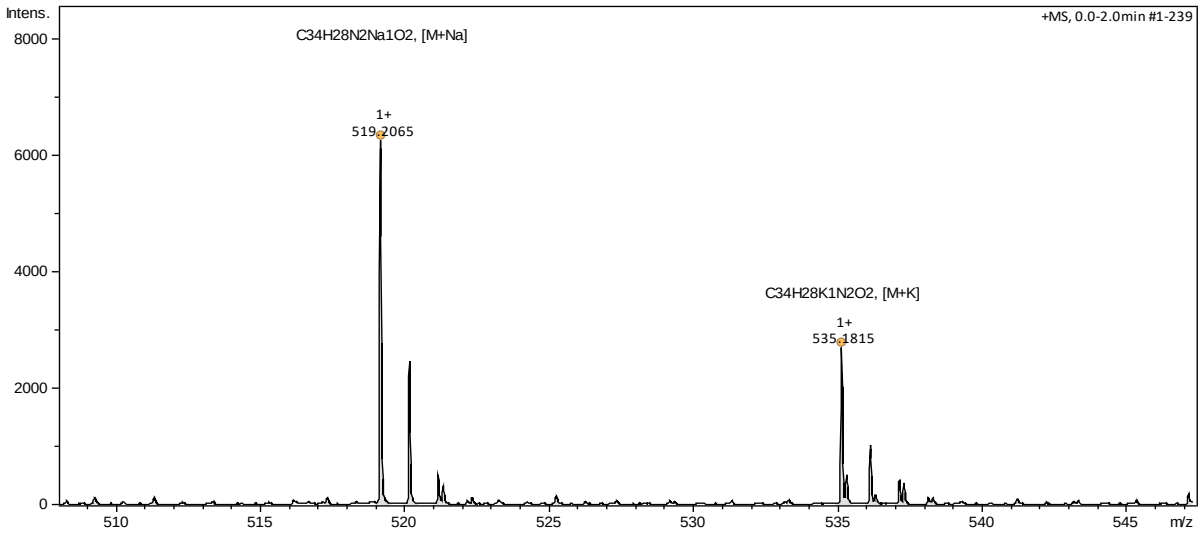

Supplementary Figure 38: HR-ESI MS spectrogram (508-547 m/z) of perylene monoimide primary amine.

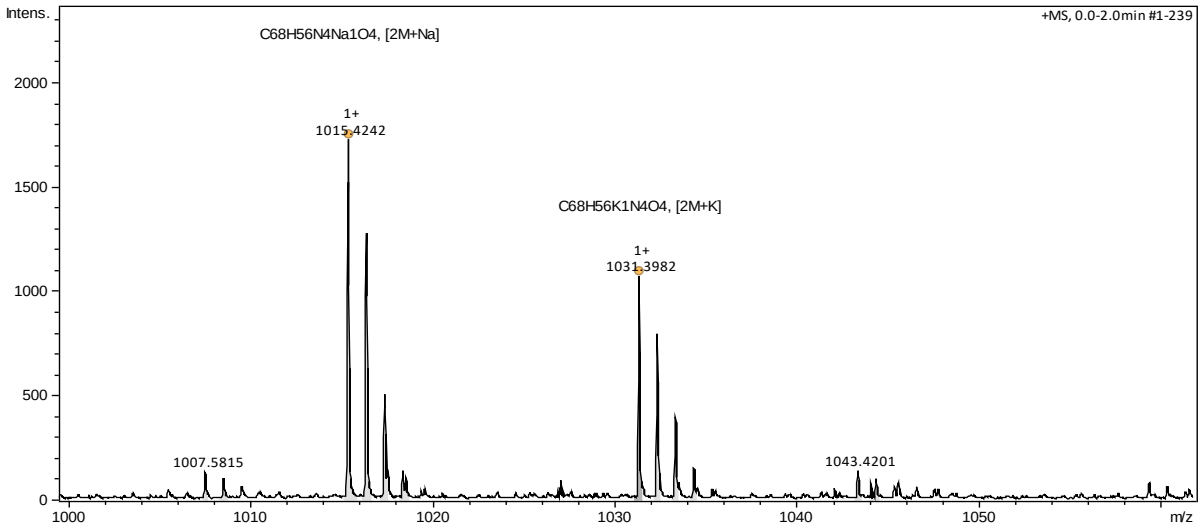

Supplementary Figure 39: HR-ESI MS spectrogram (1000-1060 m/z) of perylene monoimide primary amine.

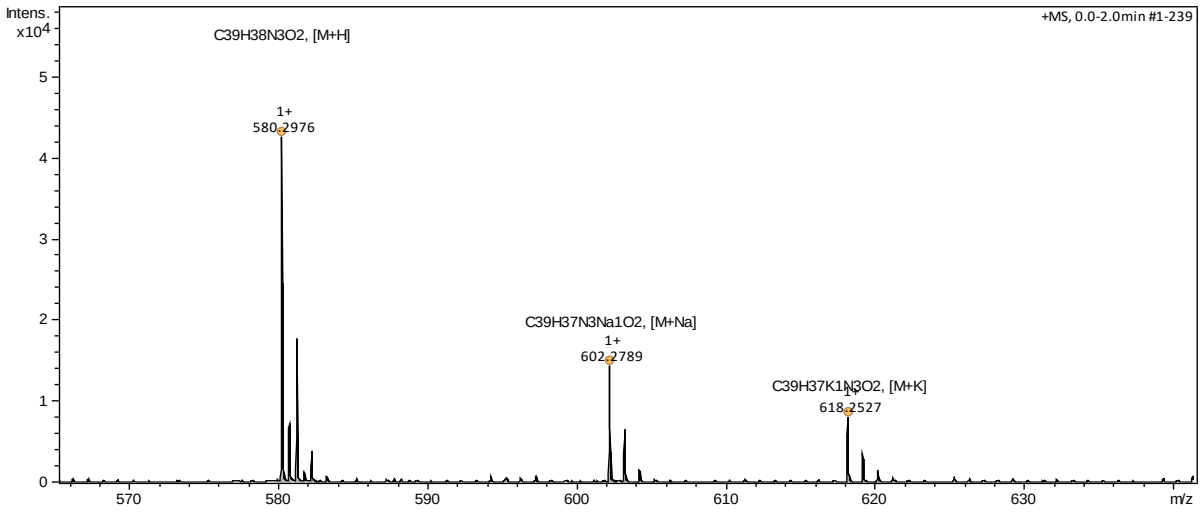

Supplementary Figure 40: HR-ESI MS spectrogram (565-645 m/z) of perylene monoimide tertiary amine.

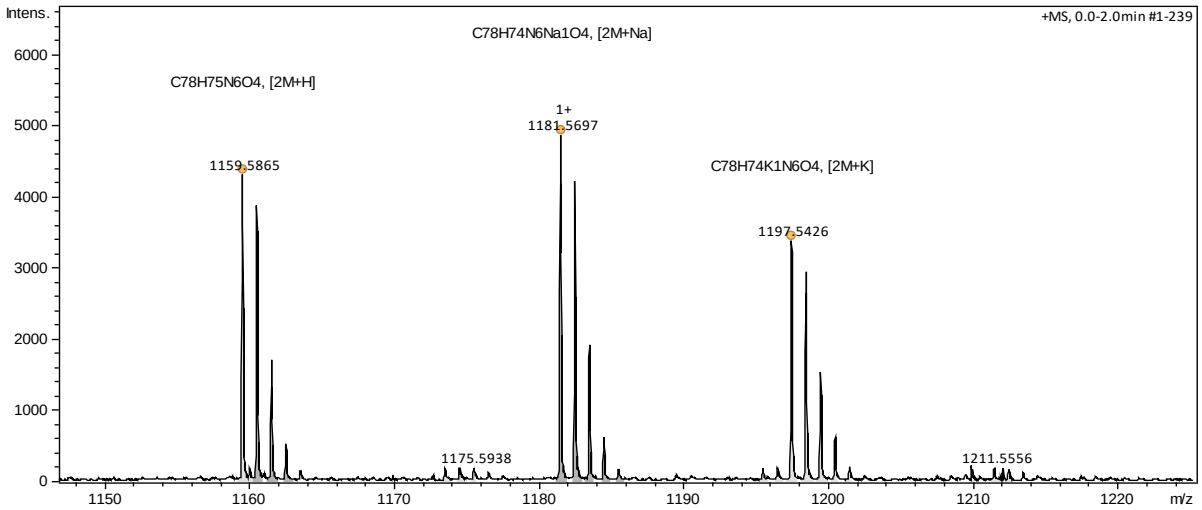

Supplementary Figure 41: HR-ESI MS spectrogram (1147-1225 m/z) of perylene monoimide tertiary amine.

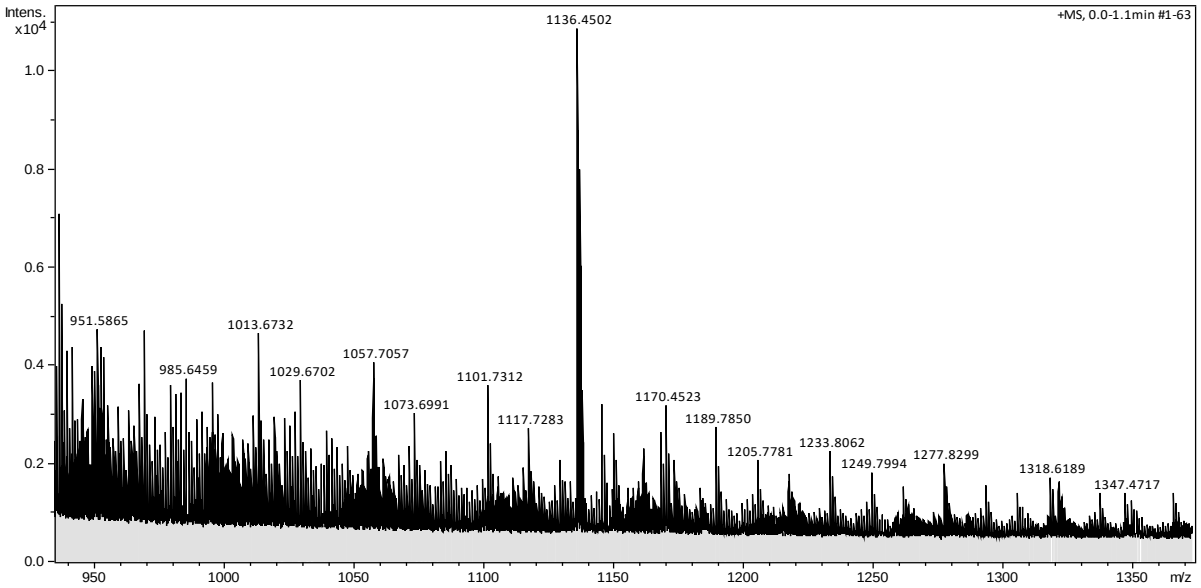

Supplementary Figure 41: HR-ESI MS spectrogram (935-1375 m/z) of the [2]rotaxane.

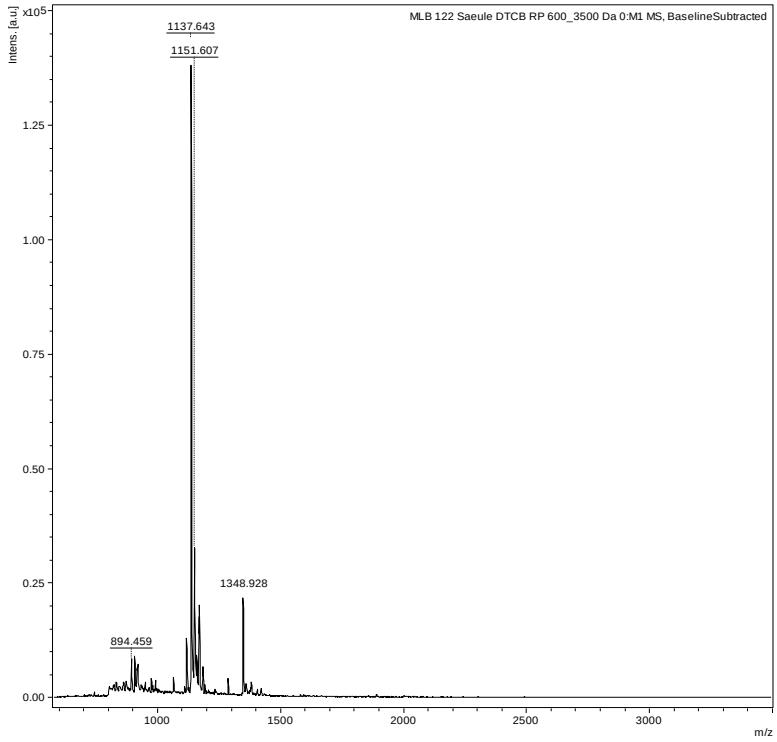

Supplementary Figure 43: MALDI-ToF MS spectrogram of the [2]rotaxane.

3.3. SEC elugrams

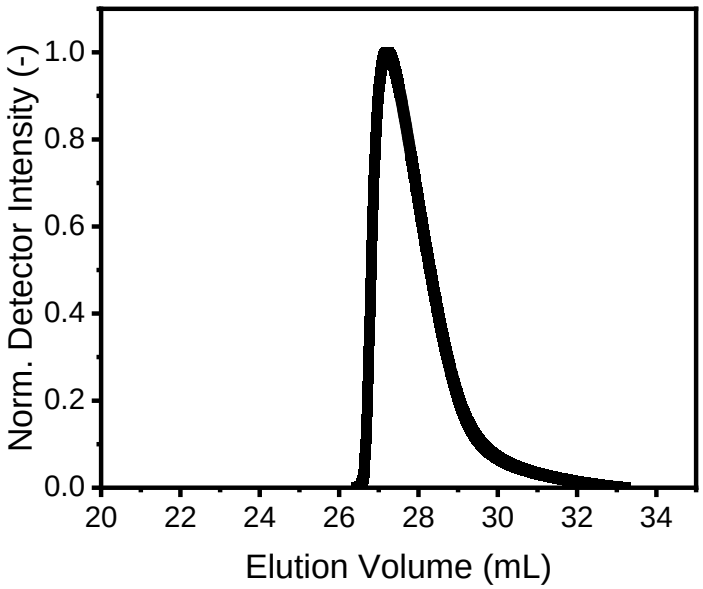

Supplementary Figure 44: SEC elugram (normalized detector intensity vs. elution volume) of mechanoresponsive POEGA polymer in THF.

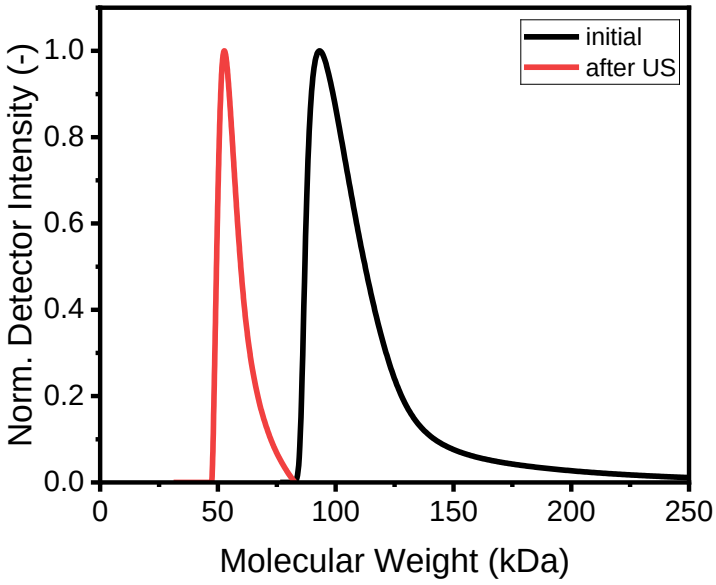

Supplementary Figure 45: Molecular weight distributions of POEGA polymer before (black, M_n = 106 kDa) and after 2 h ultrasonication (red, M_n = 56.2 kDa), determined by SEC in THF.

4. References

1. Ren, Y. & You, L. Dynamic signaling cascades: reversible covalent reaction-coupled molecular switches. *J. Am. Chem. Soc.* **137,** 14220–14228; 10.1021/jacs.5b09912 (2015).
2. Xuan, M. *et al.* Polymer Mechanochemistry in Microbubbles. *Adv. Mater.* **35,** e2305130; 10.1002/adma.202305130 (2023).
3. Montoya, L. A. & Pluth, M. D. Selective turn-on fluorescent probes for imaging hydrogen sulfide in living cells. *Chem. Comm.* **48,** 4767–4769; 10.1039/c2cc30730h (2012).
4. Mengji, R., Acharya, C., Vangala, V. & Jana, A. A lysosome-specific near-infrared fluorescent probe for in vitro cancer cell detection and non-invasive in vivo imaging. *Chem. Commun.* **55,** 14182–14185; 10.1039/c9cc07322a (2019).
5. Altaş, A. *et al.* Bay- and peri-functionalized donor-acceptor perylene monoimides via nitration and nucleophilic substitution/reduction pathway. *Mater. Today Chem.* **24,** 100908; 10.1016/j.mtchem.2022.100908 (2022).
6. Biagini, C. *et al.* Dissipative Catalysis with a Molecular Machine. *Angew. Chem. Int. Ed.* **58,** 9876–9880; 10.1002/anie.201905250 (2019).